JOINT TRANSPORTATION
RESEARCH PROGRAM
INDIANA DEPARTMENT OF TRANSPORTATION
AND PURDUE UNIVERSITY

# Pile Driving Analysis for Pile Design and Quality Assurance

Rodrigo Salgado, Vibhav Bisht, Monica Prezzi

SPR-3407 • Report Number: FHWA/IN/JTRP-2017/15 • DOI: 10.5703/1288284316514

## RECOMMENDED CITATION

Salgado, R., Bisht, V., & Prezzi, M. (2017). *Pile driving analysis for pile design and quality assurance* (Joint Transportation Research Program Publication No. FHWA/IN/JTRP-2017/15). West Lafayette, IN: Purdue University. https://doi.org/10.5703/1288284316514

## AUTHORS

**Rodrigo Salgado, PhD**
Charles Pankow Professor in Civil Engineering
Lyles School of Civil Engineering
Purdue University
(765) 494-5030
salgado@purdue.edu
*Corresponding Author*

**Vibhav Bisht**
Graduate Research Assistant
Lyles School of Civil Engineering
Purdue University

**Monica Prezzi, PhD**
Professor of Civil Engineering
Lyles School of Civil Engineering
Purdue University
(765) 494-5034
mprezzi@purdue.edu
*Corresponding Author*

## ACKNOWLEDGMENTS

The assistance of JTRP staff and, in particular, the support received from INDOT technical staff and the Study Advisory Committee members is much appreciated. The authors are also thankful for the continuous support received from the project administrator, Mr. Timothy Wells, and the business owner, Mr. Athar Khan, as well as the support received from the SAC members, Mr. Mir Zaheer and Mr. Jose Ortiz.

## JOINT TRANSPORTATION RESEARCH PROGRAM

The Joint Transportation Research Program serves as a vehicle for INDOT collaboration with higher education institutions and industry in Indiana to facilitate innovation that results in continuous improvement in the planning, design, construction, operation, management and economic efficiency of the Indiana transportation infrastructure. https://engineering.purdue.edu/JTRP/index_html

Published reports of the Joint Transportation Research Program are available at http://docs.lib.purdue.edu/jtrp/.

## NOTICE



## COPYRIGHT


Print ISBN: 978-1-62260-479-1

**TECHNICAL REPORT STANDARD TITLE PAGE**

| 1. Report No. | 2. Government Accession No. | 3. Recipient's Catalog No. |
|---|---|---|
| FHWA/IN/JTRP-2017/15 | | |

| 4. Title and Subtitle | 5. Report Date |
|---|---|
| Pile Driving Analysis for Pile Design and Quality Assurance | August 2017 |
| | 6. Performing Organization Code |

| 7. Author(s) | 8. Performing Organization Report No. |
|---|---|
| Rodrigo Salgado, Vibhav Bisht, Monica Prezzi | FHWA/IN/JTRP-2017/15 |

| 9. Performing Organization Name and Address | 10. Work Unit No. |
|---|---|
| Joint Transportation Research Program<br>Purdue University<br>550 Stadium Mall Drive<br>West Lafayette, IN 47907-2051 | 11. Contract or Grant No.<br>SPR-3407 |

| 12. Sponsoring Agency Name and Address | 13. Type of Report and Period Covered |
|---|---|
| Indiana Department of Transportation<br>State Office Building<br>100 North Senate Avenue<br>Indianapolis, IN 46204 | Final Report |
| | 14. Sponsoring Agency Code |

**15. Supplementary Notes**
Prepared in cooperation with the Indiana Department of Transportation and Federal Highway Administration.

**16. Abstract**

Driven piles are commonly used in foundation engineering. The most accurate measurement of pile capacity is achieved from measurements made during static load tests. Static load tests, however, may be too expensive for certain projects. In these cases, indirect estimates of the pile capacity can be made through dynamic measurements. These estimates can be performed either through pile driving formulae or through analytical methods, such as the Case method.

Pile driving formulae, which relate the pile set per blow to the capacity of the pile, are frequently used to determine whether the pile has achieved its design capacity. However, existing formulae have numerous shortcomings. These formulae are based on empirical observations and lack scientific validation. This report details the development of more accurate and reliable pile driving formulae developed from advanced one-dimensional FE simulations. These formulae are derived for piles installed in five typical soil profiles: a floating pile in sand, an end-bearing pile in sand, a floating pile in clay, an end-bearing pile in clay and a pile crossing a normally consolidated clay layer and resting on a dense sand layer. The proposed driving formulae are validated through well-documented case histories of full-scale instrumented driven piles. The proposed formulae are more accurate and reliable on average than other existing methods for the case histories considered in this study.

This report also discusses the development of a pile driving control system, a fully integrated system developed by Purdue that can be used to collect, process, and analyze data to estimate the capacities of piles using the Case method and the pile driving formulae developed at Purdue.

| 17. Key Words | 18. Distribution Statement |
|---|---|
| dynamic measurements, pile resistance, pile driving formulae, Case analysis | No restrictions. This document is available to the public through the National Technical Information Service, Springfield, VA 22161. |

| 19. Security Classif. (of this report) | 20. Security Classif. (of this page) | 21. No. of Pages | 22. Price |
|---|---|---|---|
| Unclassified | Unclassified | 25 | |

**Form DOT F 1700.7 (8-69)**

# EXECUTIVE SUMMARY

# PILE DRIVING ANALYSIS FOR PILE DESIGN AND QUALITY ASSURANCE

## Introduction

Dynamic measurements are often used to predict the capacity of a pile in the form of (a) pile driving formulae that relate the pile set per blow to the capacity of the pile or (b) analytical methods such as the Case method that predict the pile capacity from the accelerations and strains measured at the pile head. However, accurate prediction of pile capacity remains a challenge due to the complex response of piles during driving, prevailing uncertainties in the response of piles under static loading conditions post driving, and uncertainties stemming from simplifications made in the development of existing formulae.

For this study, a fully integrated pile driving control system (PDCS) prototype was developed that collects, processes, and analyzes dynamic data. To develop pile driving formulae, advanced and realistic soil models that explicitly consider important parameters, such as soil and pile variability, were used to accurately simulate the hammer-pile-soil system during driving and to predict the capacity of piles under static loading conditions after driving. The integrated PDCS collects dynamic data through sensors and modules during pile driving operations. The system conforms to all requirements specified in the pertinent ASTM standard (ASTM D4945). The PDCS uses wireless signals for the transmission of data collected in a PC located at a suitable distance from the driving operation. The PDCS can estimate the capacity of a single pile using existing dynamic methods, e.g., the Case method, or through the pile driving formulae developed at Purdue University.

## Findings

Comparisons between the capacities predicted using the pile driving formulae developed at Purdue and existing formulae, including the modified-Gates formula used by INDOT, for several well-documented case histories of full-scale instrumented driven piles have revealed that the pile driving formulae developed at Purdue perform better on average than other formulae. As a result, an intelligent QA/QC program for piling can use this new tool for a subset of routine piling projects, reserving other approaches for larger projects.

## Implementation

The PDCS has been subject to very limited field testing (development was done in the laboratory). Additional testing is necessary to determine the robustness and reliability of the first integrated PDCS prototype. An ideal testing scheme would be to test the system for a variety of hammer systems, pile types, and soil profiles and to compare the capacities predicted from the PDCS using the Case method and the pile driving formulae to capacities measured in fully instrumented static load tests.

CONTENTS

# LIST OF TABLES

# LIST OF FIGURES

# 1. INTRODUCTION

## 1.1 Background

Pile resistances must exceed required resistance levels (as dictated by structural loadings); however, if resistances exceed requirements by large margins, projects result uneconomical. The most important goal of QA/QC is then to allow contractors to install piles that owners can verify to be reliably but not excessively above specified resistances. This can be accomplished through pile load testing.

Pile load testing in the field adds to the overall cost of projects. Both static and dynamic tests can and are done with different frequencies on production piles. The costliest but also the most reliable are static pile load tests on instrumented piles. Dynamics tests include both pile monitoring during driving (for driven piles) and re-strike tests (tests done some time after pile installation). Although simpler in concept, static load tests tend to be reserved for large projects. A less expensive alternative that can offer real-time estimation of pile static resistance are dynamic pile load tests, which can be performed during pile driving (pile driving monitoring) but also at any time after pile installation as re-strike tests. Pile monitoring consists of recording the pile acceleration and axial strain at the pile head during driving. The pile head velocity histories can be extracted from the recorded acceleration history through numerical integration. The recorded strain is used for calculating the axial force history at the pile head. This information can be used to deduce the static pile capacity. In pile re-strike tests, the pile head is struck by a hammer after it has been fully driven into the ground. Determination of the pile capacity from static pile tests is simple, direct and straightforward. Pile capacity estimation from dynamic tests has always been more challenging, requiring a dynamic analysis that provides a link between the measurements during pile driving and the static pile resistance.

An accurate, precise relationship between measurements during pile driving and static resistance can provide simplicity and economy to piling projects, allowing engineers to monitor pile driving and indicate to a contractor or inspector that the static resistance requirements have been met before driving of a pile is stopped, avoiding overdriving while at the same time providing confidence in that the required pile capacities will be available. Additionally, reprocessing of the data in the office can provide refined estimates of static pile resistance and flag any piles as potentially defective ones. These goals can best be attained through the development of a system that allows the collection, processing and analysis of data.

## 1.2 Problem Statement Summary

A significant amount of piling work is carried out by INDOT, necessitating the usage of economical and reliable methods to ensure that (1) piling is done economically (no significant overdriving takes place) and (2) safety is not compromised (no significant under driving takes place). The accommodation of these requisites requires the development of a system that is flexible, meaning that it can be developed further to accommodate what engineers and researchers learn with additional work and research on its use, and simple to use, with the implication that engineers will be able to use it without having to face a steep learning curve.

## 1.3 Objectives and Organization

The main goal of the research is the development of the method and modified analysis, with the prototype system being a means to an end. In Chapter 2, we describe the methodology for the development of the pile driving formulae and show that they outperform existing formulae on average in predicting pile capacities from instrumented full-scale static pile load tests. In fact, they perform better than dynamic load testing for the case histories considered. In Chapter 3, we discuss the configuration and features of the pile driving control system. The operation of the system is explained to provide guidance to the operator. Chapter 4 provides a summary of the results and conclusion obtained from this study.

# 2. PILE DRIVING FORMULAE

## 2.1 Introduction

The complex interactions between the hammer, cushion, pile and soil, coupled with the significant changes in the state of the soil around the pile imposed by the driving process, makes the reliable estimation of pile capacity a difficult task. One of the tools used to assess whether a pile has reached the required capacity are the pile driving formulae. Pile driving formulae, which relate the pile set per blow to the capacity of the pile, have been used extensively due to their simplicity and economic advantages. Approximately 80% of projects in the Indiana Department of Transportation (INDOT) lack resources for dynamic testing and thus use pile driving formulae (Salgado & Zhang, 2012). Traditionally, pile driving formulae are developed based on energy conservation principles—the energy of the hammer (ram) on impact, after considering energy losses on impact from the various driving components between the hammer and the pile head, is equal to the work done by the total pile resistance for the observed pile displacement after a blow, plus any energy losses on account of dissipation inside the pile and soil. This can be expressed mathematically as:

$$e_h W_H H = Q_{ult}(s + s_c) \tag{2.1}$$

where $W_H$ is the hammer (ram) weight; $H$ is the hammer drop height; $e_h$ is the hammer efficiency; $Q_{ult}$ is the ultimate pile capacity; $s$ is the observed pile set; and $s_c$ is an empirical constant expressing the aforementioned energy losses.

TABLE 2.1
**Traditional pile driving formulas.**

| Formula | Equations[1] | Notes |
|---|---|---|
| Modified-Gates formula | $Q_u = 1.75\sqrt{E_h}(\log N - 100)$ | $E_h$ in ft-lbf |
| Modified ENR | $Q_u = \frac{1}{1000}\left(\frac{1.25 e_h E_h}{s + C/12}\right)\left(\frac{W_H + n^2 W_P}{W_H + W_P}\right)$ | $C$ = 0.1 in<br>$n$ = 0.5 for steel-on-steel anvil on steel or concrete piles |
| Danish formula | $Q_u = \frac{e_h E_h}{s + C_1}$<br>$C_1 = \sqrt{\frac{e_h E_h L}{2AE}}$ | |
| Pacific Coast Uniform Building Code (PCUBC) formula[2] | $Q_u = \frac{e_h E_h C_1}{s + C_2}$<br>$C_1 = \frac{W_H + k W_P}{W_H + W_P}$<br>$C_2 = \frac{Q_u L}{AE}$ | All symbols in SI units<br>$k$ = 0.25 for steel piles and 0.1 for all other piles |
| Janbu | $Q_u = \frac{e_h E_h}{K_u s}$<br>$C_d = 0.75 + 0.15\frac{W_P}{W_H}$<br>$K_u = C_d\left(1 + \sqrt{1 + \frac{\lambda}{C_d}}\right)$<br>$\lambda = \frac{e_h E_h L}{AEs^2}$ | |

[1]Units unless explicitly specified: $Q_u$ = predicted pile capacity (in kips), $e_h$ = hammer efficiency; $E_h$ = maximum driving energy of the hammer (in kip-ft); $N$ = number of hammer blows for 1 in. of pile set; $s$ = observed pile set in ft; $W_H$ = weight of the ram (in kips); $W_P$ = weight of the pile (in kips); $L$ = length of the pile (in ft); $A$ = cross-sectional area of the pile (in ft$^2$); $E$ = Young's modulus of the pile (in kips/ft$^2$).

[2]The calculation of predicted static capacity using PCUBC formula requires iterations.

Equation 2.1 is solved by entering the observed pile set $s$ as input and computing the pile capacity $Q_{ult}$. Several pile driving formulae are based on this approach, albeit with varying simplifying assumptions and empirical adjustments. Available pile driving formulae in the literature, among others, include the modified-Gates formula used by INDOT (2016), the modified ENR (1965) formula, the Danish formula (Olson & Flaate, 1967), the Janbu formula (Bowles, 1996) and the Pacific Coast Uniform Building Code (PCUBC) formula (Bowles, 1996). These formulae are listed in Table 2.1, and will be used for comparisons later in in this report.

Despite being important factors determining response to driving, existing formulae do not explicitly account for the soil type (e.g., sand or clay) surrounding the pile or the pile type (e.g., floating pile or end-bearing pile). Consequently, the predictions from pile driving formulae are often inaccurate and unreliable (McVay, Birgisson, Zhang, Perez, & Putcha, 2000). A critique of these formulae can be found in Likins, Fellenius, and Holtz (2012). These shortcomings of pile driving formulae are accounted for by using factors of safety, recommendations of which may be as large as six (Bowles, 1996). Salgado (2008) notes that large recommended factors of safety often diminish the advantages offered by existing formulae in deep foundation quality control. Thus, there exists a need for improved pile driving formulas exhibiting greater reliability and accuracy that would consequently require smaller factors of safety.

In this report, the pile driving process is simulated using the soil reaction models developed by Salgado, Loukidis, Abou-Jaoude, and Zhang (2015). Pile driving formulae are then developed based on the results from a series of parametric simulations for five general cases: piles in uniform sand deposits, floating piles in clay, end-bearing piles in sand, end-bearing piles in clay and piles crossing soft clay and bearing on sand. These are validated by comparing the results from well-documented case histories of static load tests on driven piles and their performance is compared with existing formulas listed in Table 2.1. The next section details the soil reaction model and the methodology used for the development of the pile driving formulae.

## 2.2 Soil Reaction Model

An advanced soil model was developed by Salgado et al. (2015) that explicitly took into account soil nonlinearity and hysteresis in order to accurately capture the complex states of soil during pile driving, and contained input parameters with a physical meaning. These models were validated by comparing their prediction with measured pile driving data for two fully instrumented, full-scale pile load tests.

The driving process was analyzed using one-dimensional analysis. The pile was discretized into segments, each of which contained a commensurate proportion of the mass of the pile, and was connected to the segments above and below via linear elastic springs that

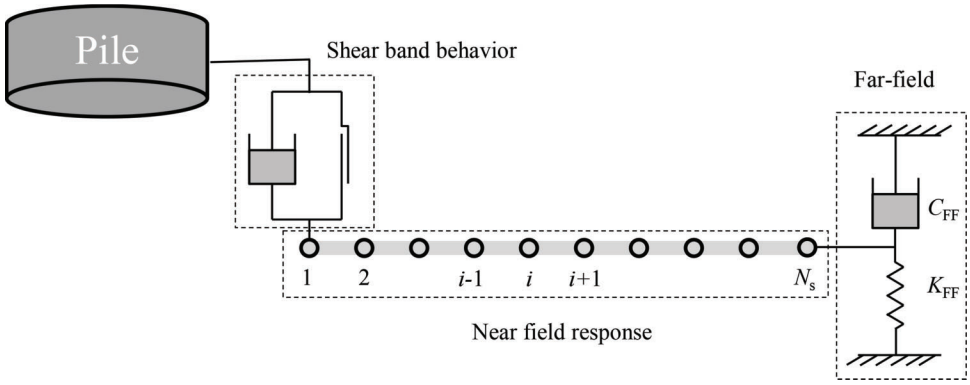


**Figure 2.1** Shaft reaction model consisting of three parts: rheological shear band model at the soil-pile interface, a near-field continuum and far-field consistent spring and radiation dashpot (after Salgado et al., 2015).

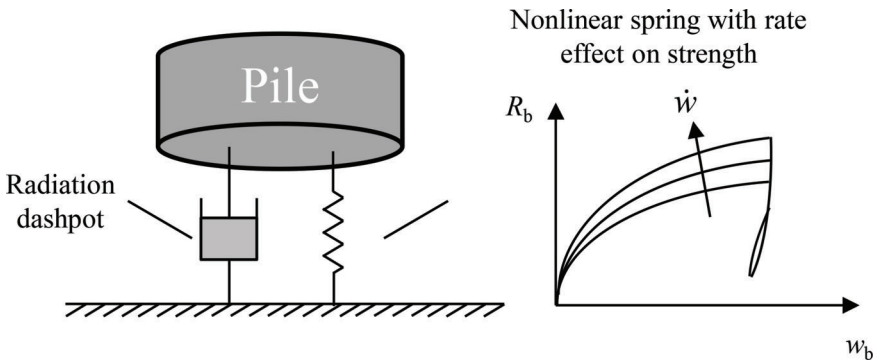


**Figure 2.2** Base reaction model consisting of a nonlinear spring and a radiation dashpot attached in parallel (after Salgado et al., 2015).

model the axial stiffness of the pile. Since the pile helmets and cushion were not modelled explicitly, the impact of the hammer was modelled by an instantaneous application of a velocity corresponding to the energy transferred from the hammer to the pile that was calculated by considering all energy losses stemming from the impact process. The energy losses could be computed from the dynamic measurements during dynamic load tests and, for all practical purposes, are equal to the hammer energy transfer ratio (ETR). ETR values can take a range of values that vary with the type of the hammer and the type of the pile being driven. According to the Rausche (2000) database, the average ETR values for drop hammers is 0.55, whereas the average ETR for diesel hammers, single acting air/steam hammers, and hydraulic hammers varies from 0.25 to 0.8.

The reaction model for the soil surrounding the shaft, shown in Figure 2.1, contains three components: (1) a rheological model representing the thin shear band formed between the interface of the pile and the soil; (2) a continuum soil disk representing the near field soil surrounding the shaft of the pile; and (3) far-field-consistent boundaries placed at the outer boundary of the soil disk. The rheological model is adopted from the work of Randolph and Simons (1986). It consists of a viscous dashpot and a plastic slider connected in parallel to each other. Sliding initiates at the pile-soil interface when the stress $\tau_s$ exceeds the unit limit shaft resistance $q_{sL}$. Until sliding initiates, the stress in the soil at the pile-soil interface is equal to the reaction force experienced by the pile at that segment, after which the viscous dashpot is activated. The viscous dashpot is a power function of the relative velocity between the pile and the first node of the near field component. The continuum approach (Honeyman, 1985) is used to capture the nonlinear stress-strain relationship of the soil in the near-field. The far field boundaries are used to absorb waves travelling radially away from the pile.

The soil reaction model at the base of the pile (Figure 2.2) consists of a non-linear spring that considers the non-linear response of the soil under the pile base and the effect of the loading rate on the base resistance, and a radiation dashpot that distinguishes between the different types of damping. The dashpot and spring are connected to each other in parallel. The non-linear spring follows a hyperbolic load-settlement relationship that is consistent with the response observed in static pile load tests. The effect of loading rates is considered by setting the limit base resistance as a power function of the base. The effects of embedment depth and hysteretic damping in the far field are considered by the damping coefficient that was calculated from FLAC simulations of an embedded oscillating footing.

## 2.3 Development of Pile Driving Formulae

A series of 1D pile driving simulations were carried out for a wished-in-place pile using the Salgado et al. (2015) model. These provide the pile set s, while the corresponding ultimate pile capacity $Q_{ult}$ values are calculated from the static design equations. The static design equations and the procedure adopted for development of the pile driving formulae are described in the section ahead.

### *2.3.1 Static Capacity Calculations*

The limit resistance $Q_L$ of an axially loaded pile is defined as the load at which the pile plunges through soil. The ultimate load $Q_{ult}$ is generally lower than $Q_L$ and depends on soil type and pile installation method. For piles in sand, the ultimate load is defined as the pile load $Q_{10\%}$ that causes a settlement at the pile head equal to 10% of its diameter $B$ (Terzaghi, 1942). For clays, except heavily overconsolidated clays, the limit resistance $Q_L$ is mobilized at settlements less than 10% (Salgado, 2008) and thus the ultimate resistance $Q_{ult}$ is practically equal to the limit resistance $Q_L$.

The ultimate pile resistance is the summation of the ultimate base resistance $Q_{b,ult}$ and limit shaft resistance $Q_{sL}$:

$$Q_{ult} = Q_{b,ult} + Q_{sL} \tag{2.2}$$

The base resistance $Q_{b,ult}$ is calculated using:

$$Q_{b,ult} = q_{b,ult} A_b \tag{2.3}$$

where $q_{b,ult}$ is the ultimate unit base resistance and $A_b$ is the area of the base of the pile.

The shaft resistance $Q_{sL}$ is calculated using:

$$Q_{sL} = \sum_i q_{sL,i} A_{s,i} \tag{2.4}$$

where $q_{sL,i}$ is the limit unit shaft resistance along the segment of the shaft intersecting the $i^{th}$ sub-layer of the soil and $A_{s,i}$ is the corresponding shaft surface area.

In this study, the Purdue design equations (Salgado, Woo, & Kim, 2011) are used for the calculation of the ultimate unit base resistance $q_{b,ult}$ and limit unit shaft resistance $q_{sL}$. For piles in sand, the following equations hold for the ultimate unit pile base resistance $q_{b,ult}$ (Salgado & Prezzi, 2007; Salgado et al., 2011):

$$\begin{aligned} &q_{b,ult} = q_{b,10\%} = (1 - 0.0058 D_R) q_{bL} \\ &q_{bL} = q_c \\ &\frac{q_c}{p_A} = 1.64 \exp\left[0.1041\phi_c + (0.0264 - 0.0002\phi_c) D_R\right] \times \left(\frac{\sigma'_h}{p_A}\right)^{0.841 - 0.0047 D_R} \end{aligned} \tag{2.5}$$

and for the unit limit shaft resistance $q_{sL}$ (Han, Prezzi, Salgado, & Zaheer, 2016):

$$\begin{aligned} &q_{sL} = K \sigma'_v \tan\delta_c \\ &K = 0.2 + (0.02 q_c/\sigma'_v - 0.2) \exp\left(-0.05 \frac{h}{B}\right) \end{aligned} \tag{2.6}$$

where $\sigma'_h$ is the *in situ* horizontal effective stress in kip/ft$^2$, $D_R$ is the sand relative density in %, $q_c$ is the cone penetration resistance in kip/ft$^2$, $p_A$ is a reference stress equal to 0.021 kip/ft$^2$, $\phi_c$ is the critical state friction angle, $\delta_c$ is the interface friction angle, which is taken as equal to $0.9\phi_c$ for steel piles and $0.95\phi_c$ for concrete piles, $K$ is the lateral earth pressure coefficient and $h$ is the distance from the pile base to the depth under consideration.

For piles in clay, the following equations hold for the calculation of the unit limit base resistance $q_{bL}$:

$$q_{bL} = N_c s_u + q_0 \tag{2.7}$$

and for the unit limit shaft resistance $q_{sL}$ (Basu, Prezzi, Salgado, & Chakraborty, 2014):

$$\begin{aligned} &q_{sL} = \alpha s_u \\ &\alpha = [A_1 + (1 - A_1) \exp\{-\left(\frac{\sigma'_{v0}}{p_A}\right)(\phi_c - \phi_{r,min})^{A_2}\}] \\ &A_1 = \begin{cases} 0.43 & \phi_c - \phi_{r,min} = 12^\circ \\ 0.75 & \phi_c - \phi_{r,min} = 5^\circ \\ 1.00 & \phi_c - \phi_{r,min} = 0^\circ \end{cases} \\ &A_2 = 0.55 + 0.43 \ln\left(\frac{s_u}{\sigma'_{v0}}\right) \end{aligned} \tag{2.8}$$

where $N_c$ is the bearing capacity factor set equal to 12.3 according to Salgado et al. (2011), $s_u$ is the undrained shear strength of the clay, $q_0$ is the soil surcharge at the pile base level and $\phi_{r,min}$ is the minimum residual friction angle of the clay. Values of $A_1$ can be obtained through linear interpolation from $\phi_c - \phi_{r,min}$ values.

### *2.3.2 Form of the Pile Driving Formula*

The pile driving formulae are developed for concrete piles and close-ended steel piles for five soil profiles (Figure 2.3). For piles in a uniform sand layer, piles crossing a normally consolidated clay layer and resting on a dense sand layer and end-bearing piles in sand, the formulas are expressed as:

$$\frac{Q_{10\%}}{p_a L^2_R} = c_1 \left(\frac{e_{eff} E_h}{W_R L_R}\right)^{c_2} \exp\left(c_3 \frac{D_R}{100\%}\right) \left(\frac{s}{L_R}\right)^{c_4} \left(\frac{W_P}{W_R}\right)^{c_5} \tag{2.9}$$

where $c_1$ - $c_5$ are dimensionless variables obtained through non-linear regression analysis described in the section ahead. For floating piles in clay and

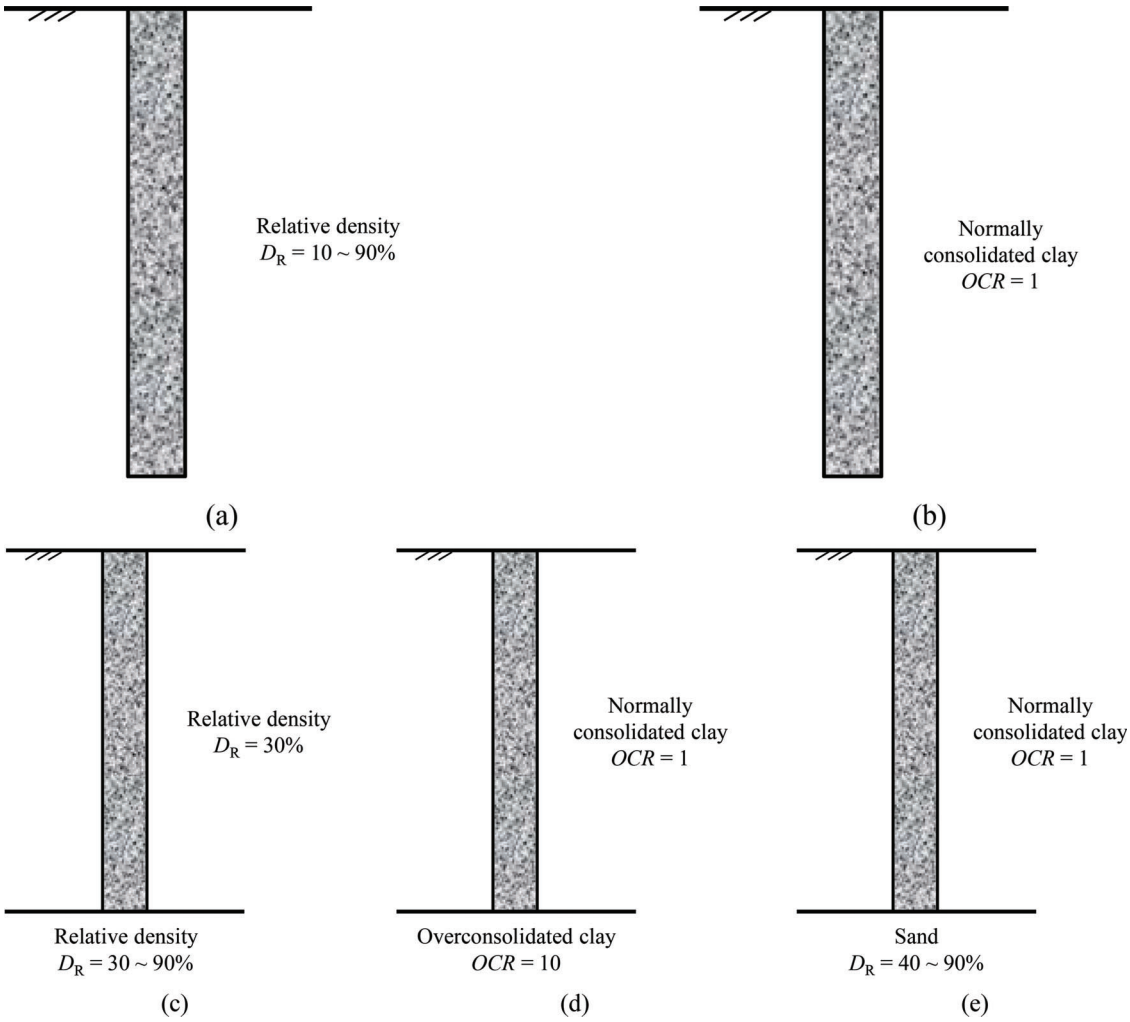


**Figure 2.3** Typical pile-soil profile systems found in pile design: (a) piles in sand of uniform density; (b) a floating pile in clay; (c) an end-bearing pile in sand; (d) an end-bearing pile in clay; (e) a pile crossing clay resting on sand.

end-bearing piles in clay, the formulae are expressed as:

$$\frac{Q_L}{p_a L^2{}_R} = c_1 \left(\frac{e_{eff} E_h}{W_R L_R}\right)^{c_2} \exp\left(c_3 \frac{s_u}{\sigma'_v}\right) \left(\frac{s}{L_R}\right)^{c_4} \left(\frac{W_P}{W_R}\right)^{c_5} \quad (2.10)$$

The formulae are similar to the form of the Janbu formula listed in Table 2.1. This can be realized by expressing the formulae, Equations 2.9 and 2.10, in the following form:

$$Q_{10\%} = \frac{e_{eff} E_h}{\left[\frac{W_R L_R}{p_a L_R{}^3} \frac{1}{c_1} \left(\frac{e_{eff} E_h}{W_R L_R}\right)^{1-c_2} \exp\left(-c_3 \frac{D_R}{100}\right) \left(\frac{s}{L_R}\right)^{-c_4-1} \left(\frac{W_P}{W_R}\right)^{-c_5}\right] \times s} = \frac{e_{eff} E_h}{A \times s} \quad (2.11)$$

$$Q_L = \frac{e_{eff} E_h}{\left[\frac{W_R L_R}{p_a L_R{}^3} \frac{1}{c_1} \left(\frac{e_{eff} E_h}{W_R L_R}\right)^{1-c_2} \exp\left(-c_3 \frac{s_u}{\sigma'_v}\right) \left(\frac{s}{L_R}\right)^{-c_4-1} \left(\frac{W_P}{W_R}\right)^{-c_5}\right] \times s} = \frac{e_{eff} E_h}{B \times s} \quad (2.12)$$

It can be seen from Equations 2.11 and 2.12 that, unlike most formulas, which add a portion of the energy lost to the final set *s,* both the Janbu formula and the formula presented in this study express this energy loss as the set *s* multiplied by a factor; $K_u$ in the case of the Janbu formula and $A$ or $B$ in the proposed formula. The formulae, however, differ on the key point of including soil properties as variables, namely $D_R$ for sands and $s_u$ for clays, which is a novelty of the proposed formulae. These variables are expected to be known or estimated from the field investigation report that typically precedes pile installation.

### *2.3.3 Procedure Adopted in the Parametric Study and Its Results*

The parameters $c_1 - c_5$ contained in Equations 2.9 and 2.10 were determined through non-linear regression analysis from an extensive parametric analysis that varied the pile dimensions, the hammer energy and the soil profile.

TABLE 2.2
**Soil parameters for typical soil profiles.**

| Case | Shaft parameter | Values of shaft parameter | Base parameter | Values of base parameter |
|---|---|---|---|---|
| Piles in sand of uniform density | Relative density $D_R$ (%) | 10, 20, 30, 40, 50, 60, 70, 80, 90 | Relative density $D_R$ (%) | same as for shaft |
| End-bearing piles in sand | Relative density $D_R$ (%) | 30 | Relative density $D_R$ (%) | 40, 50, 60, 70, 80, 90 |
| Floating piles in clay | Overconsolidation ratio *OCR*<br>$s_u/\sigma'_v$ | 1<br>0.2, 0.23, 0.25, 0.28, 0.3 | Overconsolidation ratio *OCR*<br>$s_u/\sigma'_v$ | 1<br>same as for shaft |
| End-bearing piles in clay | Overconsolidation ratio *OCR*<br>$s_u/\sigma'_v$ | 1<br>0.2, 0.23, 0.25, 0.28, 0.3 | Overconsolidation ratio *OCR*<br>$(s_u/\sigma'_v)_{NC}$ | 10<br>same as for shaft |
| Piles crossing clay resting on sand | Overconsolidation ratio *OCR*<br>$s_u/\sigma'_v$ | 1<br>0.25 | Relative density $D_R$ (%) | 40, 50, 60<br>70, 80, 90 |

TABLE 2.3
**Hammer and pile parameters.**

| Controlling variable | Values |
|---|---|
| Normalized hammer weight: $W_H/W_R$ | 0.1, 0.2, 0.3, 0.5, 1.0, 1.5 |
| Normalized drop height: $H/L_R$ | 1.5, 2.5, 3.5, 4.5, 5.5 |
| Normalized pile length: $L/L_R$ | 10, 20, 30, 40 |
| Normalized pile diameter: $B/L_R$ | 0.178, 0.356, 0.534, 0.712, 0.89, 1.068 |
| Normalized pile wall thickness: $t_W/L_R$ (for closed-ended steel pipe pile only) | 0.0095, 0.0127, 0.0159, 0.0191 |

Note: Reference force: $W_R$ = 100 kN = $2.25 \times 10^3$ lbf = 22.5 kips; reference length: $L_R$ = 1 m = 3.28 ft = 39.3 inch.

The five soil profiles considered in the parametric study, shown in Figure 2.3 and listed in Table 2.2, are expected to approximate a majority of the soil profiles found in reality. These profiles are:

1. *Pile resting on a sand layer of uniform density:* The relative density was varied from 10% to 90%, with 90% being used for the sole purpose of setting the upper limit of the numerical results.
2. *End-bearing pile in sand:* To simulate an end-bearing pile in sand, a pile crossing a superficial loose sand layer and resting on a dense sand layer was considered. The relative density of the soil around the pile shaft was kept constant at 30% and the relative density at the base was varied from 40% to 90%.
3. *Floating pile in a normally consolidated clay layer:* The ratio of the undrained shear strength of the clay to the vertical effective stress $s_u/\sigma'_v$ was varied from 0.2 to 0.3.
4. *End-bearing pile in clay:* To simulate an end-bearing pile in clay, a pile crossing a normally consolidated clay layer and resting on an over-consolidated clay layer was considered. The overconsoldation ratio OCR was taken as 10, while the ratio of the undrained shear strength of the normally consolidated clay to the vertical effective stress $s_u/\sigma'_v$ was varied from 0.2 to 0.3.
5. *Pile crossing a normally consolidated clay layer and resting on a relatively dense sand layer:* The relative density of the sand was varied from 40% to 90%, while the ratio of the undrained shear strength of the normally consolidated clay to the vertical effective stress $s_u/\sigma'_v$ was taken as 0.25.

The variables considered for the pile (Table 2.3) were the pile length L, pile diameter B and, in the case of closed-ended steel pipe piles, pile wall thickness $t_w$. The pile lengths considered were 10 m (32.8 ft), 20 m (65.6 ft), 30 m (98.4 ft) and 40 m (131.2 ft), which are representative of the pile lengths routinely used in onshore practice. The values considered for the pile wall thickness were 9.5 mm (3/8 inch), 12.7 mm (1/2 inch), 15.9 mm (5/8 inch) and 19.1 mm (3/4 inch).

The variables considered for the hammer (Table 2.3) were its weight $W_H$ and drop height $H$. The overall efficiency factor of the driving system $e_{eff}$ for the parametric study was fixed at 0.5. The exact value of $e_{eff}$ is inconsequential as the proposed equations consider the total energy being transferred from the hammer to the pile $e_{eff}E_h$, with $E_h$ varying in the parametric study due to the variations considered for the ram weight $W_H$ and drop height $H$.

Values of $c_1$-$c_5$ in Equations 2.9 and 2.10 are determined by using non-linear least-squares regression to fit the equations for the pairs of ultimate pile capacity $Q_{ult}$ and pile set $s$ produced by the parametric analyses. These values are listed in Table 2.4 for closed-ended steel pipe piles and Table 2.5 for concrete piles. The coefficient of correlation $R^2$ achieved for the non-linear regression ranges from 0.87 to 0.996. The comparisons between the static capacities calculated from Equations 2.2 to 2.8 and the capacities predicted by the proposed formulas, the PCUBC formula and the Janbu

TABLE 2.4
**Coefficients of pile driving formulas for closed-ended steel pipe piles.**

| Case | Variable | | | | | |
|---|---|---|---|---|---|---|
| | $c_1$ | $c_2$ | $c_3$ | $c_4$ | $c_5$ | $R^2$ |
| Piles in sand of uniform density | 14.97 | 0.33 | 1.04 | -0.41 | 0.89 | 0.91 |
| End-bearing piles in sand | 8.11 | 0.41 | 0.74 | -0.53 | 0.69 | 0.87 |
| Floating piles in clay | 0.72 | 0.71 | 1.3 | -0.76 | 0.3 | 0.97 |
| End-bearing piles in clay | 1.57 | 0.59 | 1.51 | -0.67 | 0.46 | 0.96 |
| Piles cross clay resting on sand | 5.77 | 0.36 | 0.12 | -0.52 | 0.71 | 0.95 |

TABLE 2.5
**Coefficients of pile driving formulas for precast concrete piles.**

| Case | Variable | | | | | |
|---|---|---|---|---|---|---|
| | $c_1$ | $c_2$ | $c_3$ | $c_4$ | $c_5$ | $R^2$ |
| Piles in sand of uniform density | 19.97 | 0.07 | 1.73 | -0.07 | 0.79 | 0.99 |
| End-bearing piles in sand | 22.05 | 0.08 | 1.13 | -0.08 | 0.76 | 0.99 |
| Floating piles in clay | 0.96 | 0.69 | 1.82 | -0.56 | 0.28 | 0.91 |
| End-bearing piles in clay | 3.01 | 0.24 | 3.1 | -0.19 | 0.75 | 0.96 |
| Piles cross clay resting on sand | 9.5 | 0.08 | 1.56 | -0.09 | 0.77 | 0.99 |

formula, are shown in Figure 2.4 for closed-ended steel pipe piles and concrete piles.

## 2.4 Case Studies

This section assesses the performance of the pile driving formulae by comparing the ultimate capacities computed from the proposed formulae to the ultimate capacities recorded in well-documented full-scale static load tests. Six case studies containing six pile load tests were considered for closed-ended steel pipe piles, whereas five cases studies containing eight pile load tests were considered for concrete piles.

The capacities calculated from traditional and proposed pile driving formulae and the capacities measured from static load tests are provided in Table 2.6 for closed-ended steel pipe piles and Table 2.7 for precast concrete piles. A summary of the hammer, soil and pile information used in the selected cases is provided in Table 2.8.

### *2.4.1 Closed-Ended Steel Pipe Piles*

**2.4.1.1 Case 1: Paik et al. (2003)**. The test site was located at Lagrange County, Indiana. The soil profile consisted of gravelly sand down to 9.8 ft and dense gravelly sand beyond that. The groundwater table was located 9.8 ft below the soil surface. The pile being tested was a closed-ended steel pipe pile with dimensions L = 27 ft, B = 14 in and $t_w$ = 0.5 in. It was driven down to a depth of 22.5 ft by an ICE-42S single acting diesel hammer with weight $W_H$ = 4.09 kips and stroke H = 10.24 ft. The rated maximum driving energy $E_h$ was computed to be 41.9 kip-ft. The pile set at end of driving (EOD) was observed to be 0.39 in. The static pile load test was performed 3 days after EOD. The ultimate load measured at a settlement of 10% B was 337 kips.

The pile driving formula for end-bearing piles in sand was used for this case. The value of relative density used in the pile driving formula was calculated to be 80%. The ultimate pile capacity $Q_{b,10\%}$ was calculated to be 376 kips using the proposed formulas. The pile capacity calculated by the modified-Gates formula is 403 kips. CAPWAP (GRL Engineers, Inc., 1997) predicted the pile capacity to be 203 kips using restrike data performed 126 days after end of driving (Paik, Salgado, Lee, & Kim, 2003).

**2.4.1.2 Case 2: Kim et al. (2009)**. The test site was located at Jasper County, Indiana. The soil profile consisted mostly of alternating layers of clayey silts and silty clays. The groundwater table was 3.28 ft below the soil surface. The pile being tested was a closed-ended steel pipe pile with dimensions L = 60.7 ft, B = 14 in and $t_w$ = 0.5 in. It was driven down to a depth of 57 ft in a thick, very dense non-plastic silt layer. An ICE 42S single-acting diesel hammer was used. The ram had a weight $W_H$ = 4.09 kips and stroke H = 10.24 ft. The rated maximum driving energy $E_h$ was computed to be 41.9 kip-ft. The pile set at EOD was observed to be 0.35 in. The static pile load test was performed 50 days after end of driving (EOD). The ultimate load measured at a settlement of 10% B was 302 kips.

The pile driving formula for piles penetrating through clay and bearing on sand was used for this case. The value of relative density used in the pile driving formula was calculated to be 90% from the CPT log. The ultimate pile capacity $Q_{b,10\%}$ was calculated to be 288 kips using the proposed formulas. The pile capacity calculated by the modified-Gates formula is 420 kips. CAPWAP (GRL Engineers, Inc., 1997) predicted the pile capacity to be 334 kips using restrike data performed 35 days after EOD (Kim, Bica, Salgado, Prezzi, & Lee, 2003).

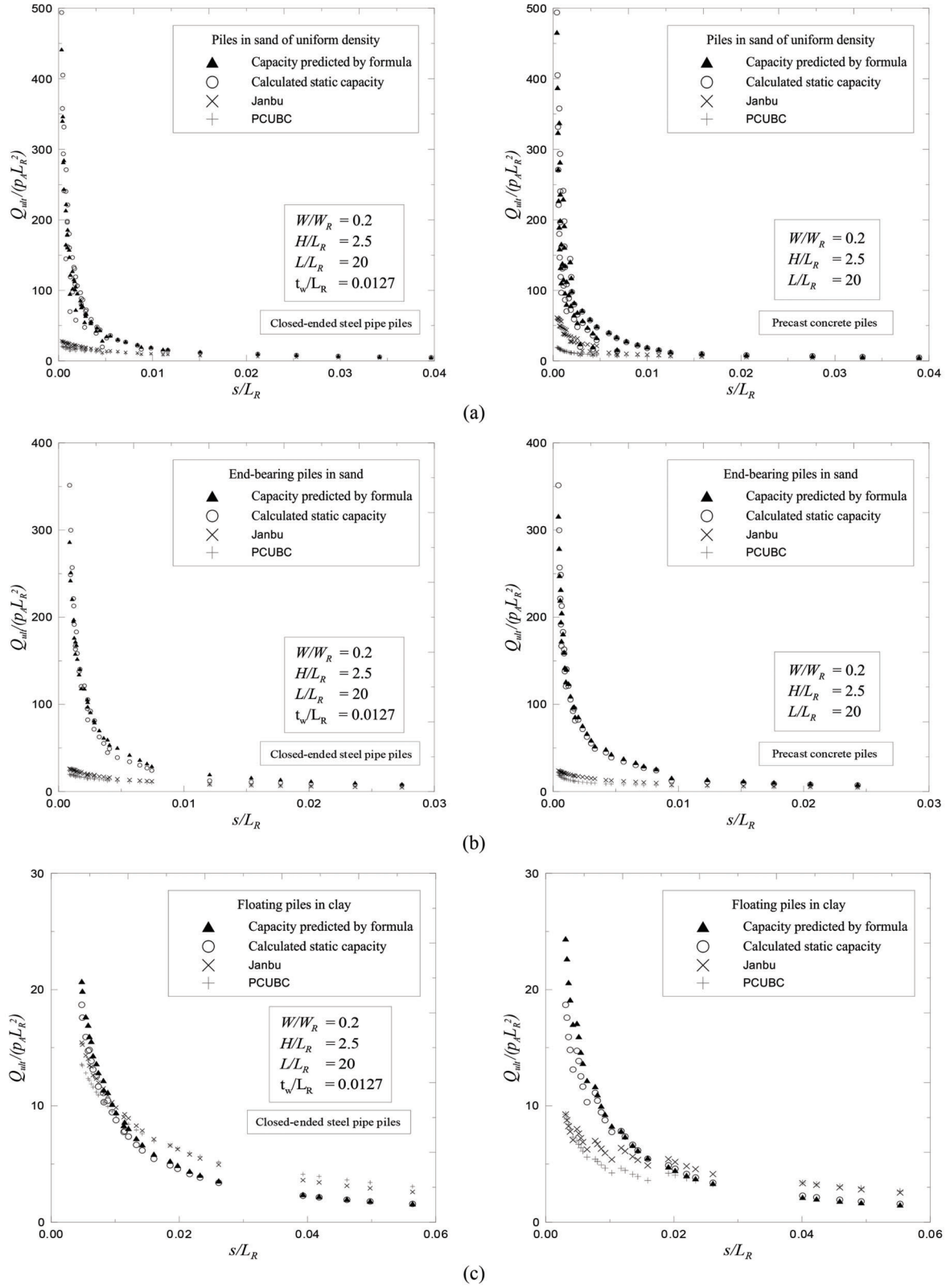


**Figure 2.4** Comparison between capacity predicted by proposed formulae, calculated static capacity, capacity predicted by Janbu formula and capacity predicted by PCUBC formula for closed-ended steel pipe piles and concrete piles: (a) piles in sand of uniform density; (b) end-bearing piles in sand; (c) floating piles in clay; (d) end-bearing piles in clay; (e) end-bearing piles crossing clay and resting on sand (after Salgado, Zhang, Abou-Jaoude, Loukidis, & Bisht, 2017).

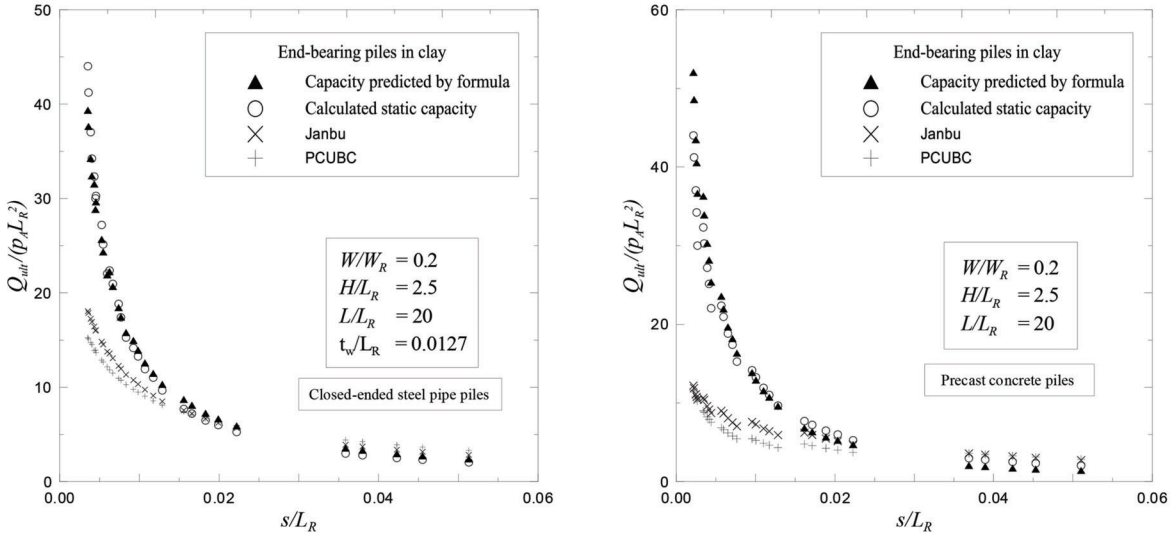


(d)

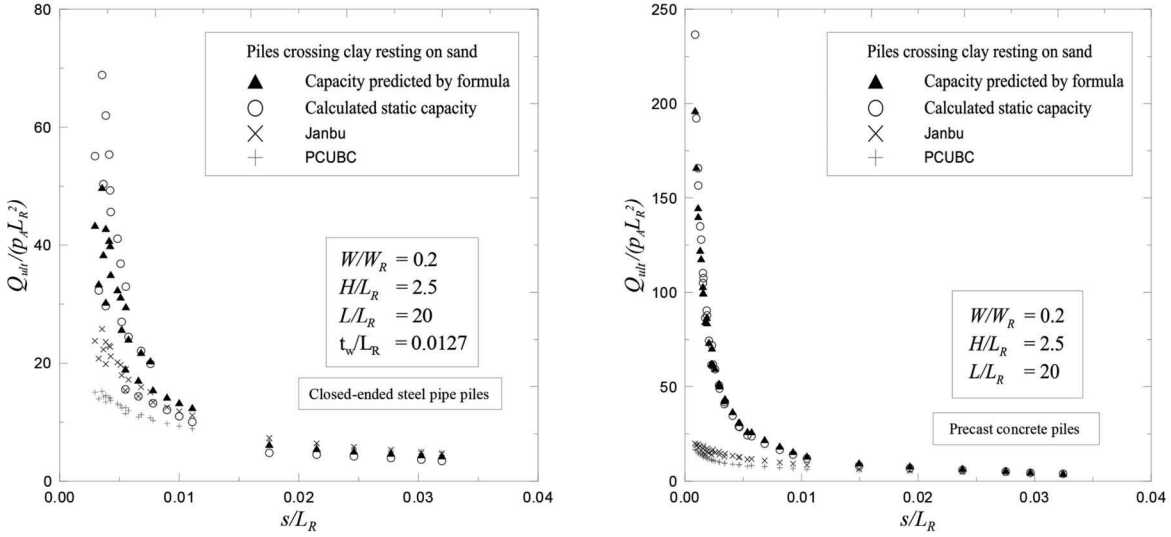


(e)

**Figure 2.4** Continued.

TABLE 2.6
**Case studies for closed-ended steel pipe piles in kips.**

| Case | Static load test | Proposed formula | CAPWAP | Modified-Gates formula | Modified ENR | Danish formula | Pacific Coast formula | Janbu formula |
|---|---|---|---|---|---|---|---|---|
| 1 | 337 | 376 | 203 | 403 | 821 | 617 | 527 | 518 |
| 2 | 302 | 288 | 334 | 420 | 737 | 515 | 362 | 414 |
| 3 | 431 | 315 | 220 | 656 | 1293 | 668 | 410 | 512 |
| 4 | 933 | 668 | N/A | 681 | 1483 | 920 | 654 | 742 |
| 5 | 227 | 145 | N/A | 409 | 822 | 544 | 497 | 463 |
| 6 | 736 | 742 | 757 | 637 | 1951 | 774 | 570 | 619 |

**2.4.1.3 Case 3: Fellenius et al. (2004)**. The test site was located at Sandpoint in Idaho. The soil profile consisted of a thick sandy layer followed by normally consolidated postglacial alluvial deposit extending to a depth of 155 ft. The groundwater table was located 13 ft below the soil surface. The pile being tested was a closed-ended steel pipe pile with dimensions L = 147.5 ft, B = 16 in and $t_w$ = 0.49 in. It was driven down to a depth of 147.5 ft by an APE D36-32 single-acting diesel hammer with weight $W_H$ = 7.94 kips and stroke H = 13.75 ft. The rated maximum driving energy $E_h$ was 109.1 kip-ft. The pile set at EOD was observed

TABLE 2.7
**Case studies for precast concrete piles: measured and estimated loads in kips.**

| Case | Static load test | Proposed formula | Modified-Gates formula | Modified ENR | Danish formula | Pacific Coast formula | Janbu formula |
|---|---|---|---|---|---|---|---|
| 6 | 255 | 341 | 290 | 473 | 355 | 299 | 302 |
| | 538 | 602 | 478 | 1231 | 676 | 493 | 579 |
| 7 | 500 | 731 | 230 | 240 | 260 | 158 | 180 |
| | 440 | 592 | 385 | 596 | 490 | 299 | 381 |
| | 940 | 950 | 733 | 1689 | 1313 | 908 | 1031 |
| 8 | 215 | 132 | 305 | 436 | 430 | 243 | 339 |
| 9 | 247 | 301 | 419 | 667 | 562 | 309 | 420 |
| 10 | 841 | 1078 | 514 | 891 | 402 | 188 | 277 |

TABLE 2.8
**Summary of hammer, pile and soil information used in the pile driving formulas in the case studies.**

| Case | Pile No. | Hammer | $W_H$ (kips) | $E_h$ (kip-ft) | $e_h$ | $e_{eff}$[1] | $W_P$ (kips) | $D_R$ (%) | $s_u/\sigma'_v$ | $s$ (in) |
|---|---|---|---|---|---|---|---|---|---|---|
| 1 | 1 | ICE 42-S | 4.1 | 41.9 | 0.85 | 0.38 | 2.0 | 80 | N/A | 0.39 |
| 2 | 2 | ICE 42-S | 4.1 | 41.9 | 0.85 | 0.38 | 4.1 | 90 | N/A | 0.35 |
| 3 | 3 | APE D36-32 | 7.9 | 109.1 | 0.85 | 0.38 | 12.0 | N/A | 0.18 | 0.49 |
| 4 | 4 | Delmag D62-22 | 13.7 | 165.4 | 0.85 | 0.38 | 13.3 | 37.5 | N/A | 0.80 |
| 5 | 5 | Delmag D30-13 | 6.6 | 66.2 | 0.85 | 0.38 | 2.1 | 85 | N/A | 0.74 |
| 6 | 6 | APE D30-32 | 6.6 | 69.4 | 0.85 | 0.38 | 2.9 | 85 | N/A | 0.25 |
| 7 | 7 | Drop hammer | 11.2 | 22.1 | 0.75 | 0.55 | 4.4 | 55 | N/A | 0.31 |
| | 8 | | 11.2 | 27.6 | 0.75 | 0.55 | 4.1 | 100 | N/A | 0.10 |
| 8 | 9 | Vulcan 010 | 10.0 | 32.5 | 0.85 | 0.4 | 13.0 | 45 | N/A | 0.90 |
| | 10 | | 10.0 | 32.5 | 0.85 | 0.4 | 12.5 | 30 | N/A | 0.31 |
| | 11 | Raymond 8/0 | 25.0 | 266.7 | 0.85 | 0.4 | 22.7 | 27 | N/A | 1.20 |
| 9 | 12 | Drop hammer | 3.3 | 9.9 | 0.75 | 0.55 | 4.5 | N/A | 0.16 | 0.05 |
| 10 | 13 | Delmag 12 | 2.8 | 34.0 | 0.85 | 0.25 | 4.7 | 40 | N/A | 0.25 |
| 11 | 14 | Drop hammer | 8.5 | 16.8 | 0.75 | 0.55 | 12.4 | 100 | N/A | 0.02 |

[1]Assumed values: 0.38 and 0.25 for diesel hammers acting on steel and concrete piles respectively (Rausche, 2000); 0.54 and 0.40 for single acting air/steam hammers on steel and concrete piles respectively (Rausche, 2000); 0.55 for drop hammers acting on either steel or concrete piles (Allen, 2005; Lam, 2007; Lim & Broms, 1990; Mostafa, 2011).

to be 0.49 in. The static load test was performed 48 days after EOD. The test pile failed in plunging at 431 kips.

The pile driving formula for a floating pile in clay was used for this case. The $\frac{s_u}{\sigma'_v}$ of the clay layer was computed to be 0.18 at the pile base. The pile capacity was calculated to be 315 kips using the proposed formulas. The pile capacity calculated by the modified-Gates formula is 656 kips. CAPWAP (GRL Engineers, Inc., 1997) predicted the pile capacity to be 220 kips using restrike data performed 1 day after end of driving (Fellenius, Harris, & Anderson, 2004). It is plausible that setup during the 47-day gap between restrike and static load test may have caused the significant under-prediction.

**2.4.1.4 Case 4: Yen et al. (1989)**. The test site was located at the southern coast of Taiwan. The soil profile consisted of a thick layer of hydraulic sand fill and natural sand underlain by a thick clay layer and a thick sand layer. The groundwater table was located 3.28 ft below the soil surface. The pile being tested was a closed-ended steel pipe pile with dimensions L = 118 ft, B = 24 in and $t_w$ = 0.47 in. It was driven down to a depth of 112 ft by a Delmag D62-22 diesel hammer with weight $W_H$ = 13.69 kips and stroke H = 12.08 ft. The rated maximum driving energy $E_h$ was 165.4 kip-ft. The pile set at EOD was observed to be 0.8 in. The ultimate load measured at a settlement of 10% B was 933 kips.

The pile driving formula for a pile crossing clay and resting on sand was used for this case. The relative

density was computed to be 41% from SPT using the Skempton (1986) equation:

$$\frac{D_R}{100\%} = \sqrt{\frac{N_{60}}{A + BC\frac{\sigma_v'}{p_A}}} \quad (2.13)$$

where $A$ is between 27 to 46; $B$ is approximately 27, and $C$ is 1 for normally consolidated sand. Using the CPT log, the relative density was computed to be 34% using the Salgado and Prezzi (2007) equation:

$$D_R = \frac{\ln\left(\frac{q_c}{p_A}\right) - 0.4947 - 0.1041\phi_c - 0.841\ln\left(\frac{\sigma_h'}{p_A}\right)}{0.0264 - 0.0002\phi_c - 0.0047\ln\left(\frac{\sigma_h'}{p_A}\right)} \quad (2.14)$$

The value of relative density used in the pile driving formula was taken as 37.5%; the average from the SPT and CPT logs. The ultimate pile capacity $Q_{b,10\%}$ was calculated to be 668 kips using the proposed formulas. The pile capacity calculated by the modified-Gates formula is 681 kips.

**2.4.1.5 Case 5: Kulesza and Fellenius (2012)**. The test site was located near Briech in Morroco. The soil profile consisted of thick fill layer underlain by a thick NC clay layer and a thick dense sand layer. The groundwater table was located 8.9 ft below the soil surface. The pile being tested was a closed-ended steel pipe pile with dimensions L = 34.5 ft, B = 16 in and $t_w$ = 3/8 in. It was driven down by a Delmag D30-13 single-acting diesel with weight $W_H$ = 6.61 kips and stroke H = 10.01 ft. The rated maximum driving energy $E_h$ was 66.2 kip-ft. The pile set at EOD was observed to be 0.74 in. The static pile load test was performed 6 years after EOD. The pile plunged at a settlement less than 0.1B on an applied load of 227 kips.

The pile driving formula for a pile crossing clay and resting on sand was used for this case. The relative density was computed to be 85% using Equation 2.14. The pile capacity was calculated to be 145 kips using the proposed formulas. The pile capacity calculated by the modified-Gates formula is 409 kips.

**2.4.1.6 Case 6: Han et al. (2016)**. The test was performed at Marshall County, Indiana, USA. The soil profile consisted of dense sand intermixed with silt to a depth of approximately 82 ft. The ground water table was located 14 ft below the ground surface. The pile being tested was a closed-ended steel pipe pile with dimensions L = 52.5 ft. It was driven down to a depth of 50.5 ft by an APE D30-32 single-acting diesel hammer. The ram had a weight $W_H$ = 6.61 kips and stroke H = 10.5 ft. The rated maximum driving energy $E_h$ was computed to be 69.4 kip-ft. The pile set at EOD was observed to be 0.25 in. The static pile load test was performed 9 days after EOD. The ultimate load measured at a settlement of 10% B was 736 kips.

The pile driving formula for a pile in sand of uniform relative density was used for this case. The relative density was computed to be 85%, averaged across the pile shaft. The ultimate pile capacity $Q_{b,10\%}$ was calculated to be 742 kips using the proposed formulas. The pile capacity calculated by the modified-Gates formula is 637 kips. CAPWAP (GRL Engineers, Inc., 1997) predicted the pile capacity to be 757 kips using restrike data performed 22 days after end of driving.

### *2.4.2 Concrete Piles*

**2.4.2.1 Case 7: Ismael (1999)**. Two tests were performed at two locations in Salmiya and Shuwaikh in Kuwait respectively. The soil profile at Salmiya consisted of fine-to-medium silty sand underlain by dense sand. The ground water table was located 6.5 ft below the ground surface. The pile being tested was a square precast concrete pile with dimensions B = 12 in. It was driven down to a depth of 30.3 ft by a drop hammer. The ram had a weight $W_H$ = 11.2 kips and stroke H = 1.97 ft. The rated maximum driving energy $E_h$ was computed to be 22.1 kip-ft. The pile set at EOD was observed to be 0.31 in. The ultimate load measured at a settlement of 10% B was 255 kips.

The pile driving formula for an end-bearing pile in sand was used for this case. The relative density was computed from SPT N values to be 55% at the pile base using Equation 2.13. The ultimate pile capacity $Q_{b,10\%}$ was calculated to be 341 kips using the proposed formulas. The pile capacity calculated by the modified-Gates formula is 290 kips.

The soil profile at Shuwaikh consisted of a fine-to-coarse sand fill underlain with fine to medium silty sand. The relative density was computed from SPT N values using Equation 2.13 to be 100% at the pile base. The ground water table was located 5 ft below the ground surface. The pile being tested was a square precast concrete pile with dimension B = 11.8 in. It was driven down to a depth of 28.5 ft by the same drop hammer as in test at Salmiya. The pile set at EOD was observed to be 0.1 in. The ultimate load measured at a settlement of 10% B was 538 kips. The pile driving formula for an end-bearing pile in sand was used for this case. The ultimate pile capacity $Q_{b,10\%}$ was calculated to be 602 kips using the proposed formulas. The pile capacity calculated by the modified-Gates formula is 478 kips.

**2.4.2.2 Case 8: Martin et al. (1987)**. The test site was located at the Tidewater region of Virginia. Three static load tests were performed on three precast concrete piles with different dimensions. The soil profile in all three cases consisted of a weak silty, clayey sand layer underlain by a loose-to-medium dense sand layer. The ground water table was located 8.2 ft below the ground surface. The first pile being tested was a square precast concrete pile with dimensions L = 69 ft, B = 14 in. It was driven down to a depth of 62 ft by a Vulcan 010 single-acting, air-driven hammer. The ram had a weight $W_H$ = 10 kips and stroke H = 3.25 ft. The rated

maximum driving energy $E_h$ was computed to be 32.5 kip-ft. The pile set at EOD was observed to be 0.9 in. The ultimate load measured at a settlement of 10% B was 500 kips.

The pile driving formula for piles in a sand of uniform density was used for this case. The relative density was computed from SPT N values using Equation 2.13 to be 45% at the pile base. The ultimate pile capacity $Q_{b,10\%}$ was predicted to be 731 kips using the proposed formulas. The pile capacity calculated by the modified-Gates formula is 230 kips.

The second pile was identical in dimensions to the same pile and was driven by the same hammer to an embedment depth of 60 ft. The pile set at EOD was observed to be 0.31 in. The ultimate load measured at a settlement of 10% B was 440 kips.

The pile driving formula for piles in a sand of uniform density was used for this case. The relative density was computed from SPT N values using Equation 2.13 to be 30% at the pile base. The ultimate pile capacity $Q_{b,10\%}$ was predicted to be 592 kips using the proposed formulas. The pile capacity calculated by the modified-Gates formula is 385 kips.

The third pile being tested was a square precast concrete pile with dimensions L = 85.3 ft, B = 18 in. It was driven down to a depth of 67 ft by a Raymond 8/0 single acting, air-driven hammer. The ram had a weight $W_H$ = 25.02 kips and stroke H = 10.66 ft. The rated maximum driving energy $E_h$ was computed to be 266.7 kip-ft. The pile set at EOD was observed to be 1.2 in. The ultimate load measured at a settlement of 10% B was 940 kips.

The pile driving formula for an end-bearing pile in sand was used for this case. The relative density was computed from SPT N values using Equation 2.13 to be 27% at the pile base. The ultimate pile capacity $Q_{b,10\%}$ was predicted to be 950 kips using the proposed formulas. The pile capacity calculated by the modified-Gates formula is 733 kips.

**2.4.2.3 Case 9: Meyerhof and Murdock (1953)**. The test site was located at the Barnet, near London. The soil profile consisted of thick soft Brown London Clay underlain by stiff Brown London Clay. The groundwater table was not found during field investigation. The pile being tested was a square precast concrete pile with dimensions L = 30 ft, B = 12 in. It was driven down to a depth of 28 ft by a drop hammer. The ram had a weight $W_H$ = 3.35 kips and stroke H = 2.95 ft. The rated driving energy $E_h$ was computed to be 9.9 kip-ft. The pile set at EOD was observed to be 0.05 in. The static pile load test was performed one month after EOD. The ultimate load measured at a settlement of 10% B was 215 kips.

The pile driving formula for a floating pile in clay was used for this case. The $\frac{s_u}{\sigma'_v}$ of the clay layer was computed to be 0.16 at the pile base. The ultimate pile capacity $Q_{b,10\%}$ was predicted to be 132 kips using the proposed formulas. The pile capacity calculated by the modified-Gates formula is 305 kips.

**2.4.2.4 Case 10: Altaee et al. (1992)**. The test site was located at Baghdad University Complex, Iraq. The soil profile consisted of a 3-m-thick clayey silty sand layer underlain by a thick uniform sand layer with some silt. The ground water table was located 21 ft below the ground surface. The pile being tested was a square precast concrete pile with dimensions L = 12.0 m, B = 285 mm. It was driven down to a depth of 36 ft by a Delmag D12 diesel hammer. The ram had a weight $W_H$ = 2.83 kips and stroke H = 12 ft. The rated driving energy $E_h$ was computed to be 34.0 kip-ft. The pile set at EOD was observed to be 0.25 in. The ultimate load measured at a settlement of 10% B was 247 kips.

The pile driving formula for an end-bearing pile in sand was used for this case. The relative density was computed to be 40% at the pile base using an average of SPT and CPT estimates. The ultimate pile capacity $Q_{b,10\%}$ was predicted to be 301 kips using the proposed formulas. The pile capacity calculated by the modified-Gates formula is 419 kips.

**2.4.2.5 Case 11: Fellenius and Samson (1976)**. The test site was located at Contrecoeur, Quebec. The soil profile consisted of thick sensitive marine clay underlain by dense silty sand. The ground water table was located 3.28 ft below the ground surface. The pile being tested was a Herkules H800 concrete pile with B = 11.8 in. It was driven down to a depth of 85.3 ft by a drop hammer. The ram had a weight $W_H$ = 8.54 kips and stroke H = 1.97 ft. The rated driving energy $E_h$ was computed to be 16.8 kip-ft. The pile set at EOD was observed to be 0.02 in. The ultimate load measured at a settlement of 10% B was 841 kips.

The pile driving formula for piles crossing a clay layer and resting on a sand layer was used for this case. The relative density was computed using Equation 2.13 to be greater than 100% at the pile base; a value of 100% was used. The ultimate pile capacity $Q_{b,10\%}$ was predicted to be 1078 kips using the proposed formulas. The pile capacity calculated by the modified-Gates formula is 514 kips.

### *2.4.3 Summary of the Pile Driving Formula Performance*

Two performance measures were used to assess and compare the performance of the proposed formulas with the existing formulas. The first measure used is the average $r_Q$ ratio of predicted to observed pile capacity ($r_Q = Q_{ult,predicted}/Q_{ult,observed}$). This represents the tendency of a formula to either under-predict or over-predict measured capacities. A value equal to one would indicate that the formula has no bias in under-predicting or over-predicting capacities, a value greater than one would indicate a tendency to over-predict measured capacities, and a value less than one would indicate a tendency to under-predict measured capacities. The second measure used is the Mean Absolute Percentage Error (*MAPE*):

TABLE 2.9
**$r_Q$ values for predicted pile capacities with different pile driving formulas.**

| Case | Proposed formula | CAPWAP | Modified-Gates formula | Modified ENR | Danish formula | Pacific Coast formula | Janbu formula |
|---|---|---|---|---|---|---|---|
| 1 | 1.11 | 0.60 | 1.20 | 2.44 | 1.83 | 1.56 | 1.54 |
| 2 | 0.95 | 1.10 | 1.39 | 2.44 | 1.70 | 1.20 | 1.37 |
| 3 | 0.73 | 0.51 | 1.52 | 3.00 | 1.55 | 0.95 | 1.19 |
| 4 | 0.72 | | 0.73 | 1.59 | 0.99 | 0.70 | 0.80 |
| 5 | 0.64 | | 1.80 | 3.62 | 2.40 | 2.19 | 2.04 |
| 6 | 1.01 | 1.03 | 0.87 | 2.65 | 1.05 | 0.77 | 0.84 |
| 7 | 1.33 | | 1.14 | 1.85 | 1.39 | 1.17 | 1.18 |
| | 1.12 | | 0.89 | 2.29 | 1.26 | 0.92 | 1.08 |
| 8 | 1.46 | | 0.61 | 0.48 | 0.52 | 0.32 | 0.36 |
| | 1.34 | | 0.52 | 1.35 | 1.11 | 0.68 | 0.87 |
| | 1.01 | | 0.41 | 1.80 | 1.40 | 0.97 | 1.10 |
| 9 | 0.61 | | 3.41 | 2.03 | 2.00 | 1.13 | 1.58 |
| 10 | 1.22 | | 1.69 | 2.70 | 2.27 | 1.25 | 1.70 |
| 11 | 1.28 | | 0.61 | 1.06 | 0.48 | 0.22 | 0.33 |

$$MAPE = \frac{1}{N}\sum_{i=1}^{N}\left|\frac{Q^{(i)}_{ult,predicted} - Q^{(i)}_{ult,observed}}{Q^{(i)}_{ult,observed}}\right| = \frac{1}{N}\sum_{i=1}^{N}\left|r^{(i)}_{Q} - 1\right| \quad (2.15)$$

where $N$ is the total number of case history piles. The $MAPE$ quantifies the uncertainties present in the predictions. A larger $MAPE$ value would represents larger uncertainty in the predictions of a formula.

The average $r_Q$ and $MAPE$ values are given in Table 2.9. For the proposed pile driving formulae, the ratio $r_Q$ has a value equal to 1.04 for all case histories examined, i.e., the formulas overestimate the actual pile capacity by 4% on average. The MAPE for the proposed formulas is equal to 23%. Traditional formulas produce estimates with greater uncertainty; some formulas are also strongly biased. The modified-Gates formula is slightly unconservative (Figure 2.5a) and provides dispersed predictions, with average $r_Q$=1.20 and a MAPE of 54% (Figure 2.5b). The Janbu formula is similarly slightly unconservative, with an average $r_Q$=1.14 and MAPE of 40%. The modified ENR formula and Danish formula are extremely unconservative, with average $r_Q$ of 2.09 and 1.42 and MAPE of 117% and 57% respectively. The best performance among the existing formulas considered was by the PCUBC formula, which has an average $r_Q$=1.00 and MAPE of 36%. Although the PCUBC formula has no bias, it exhibits much greater uncertainty in its predictions. This can be seen by comparing the minimum and maximum $r_Q$ values (0.22 and 2.19) of the PCUBC formula and the proposed formulas (0.61 and 1.46); the proposed formula have a much narrower range.

## 2.5 Summary and Conclusions

Pile quality assurance and control rely on tools such as pile driving formulas, dynamic load tests and static load tests, each of which have a different application domain. The pile driving formulas proposed here can be useful in routine, low- to medium-budget projects, given that they have proven reliable. This study uses predictions of 1D pile driving simulations to develop pile driving formulas that are reliable by explicitly accounting for the soil type surrounding the pile (sand or clay) and pile type (closed-ended steel pipe piles or precast concrete piles).

Eleven well-documented case histories that include thirteen static pile load tests have been used to validate the proposed pile driving formulas. The predictions provided by existing and proposed pile driving formula were compared with the results from static pile load tests. It has been shown that the proposed pile driving formulas exhibit less bias and significantly less uncertainty, for the cases in which the design soil profile can be approximated into one of the five general soil profile configurations for which the formulas were derived, than the traditional pile driving formulas commonly used in practice and indeed than dynamic load tests interpreted in the office using signal matching (through CAPWAP®).

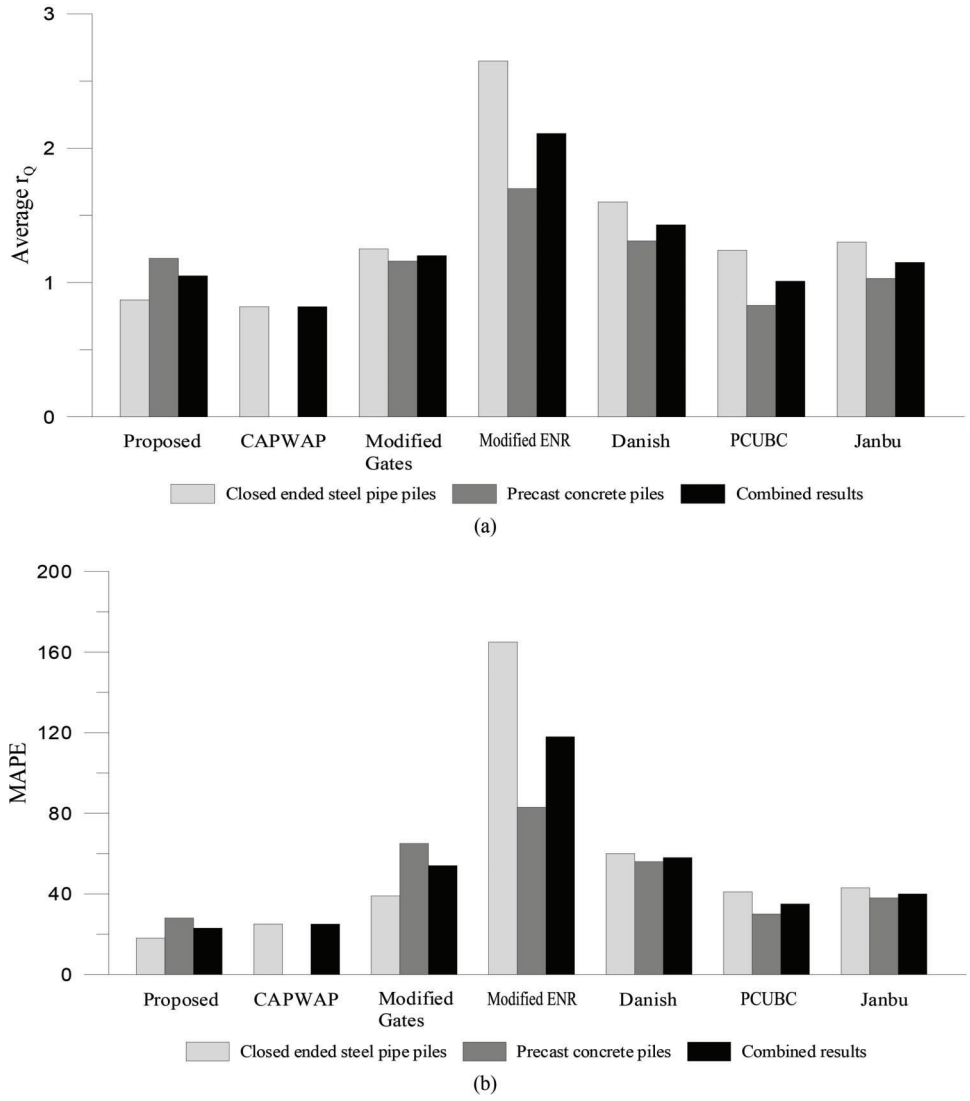


**Figure 2.5** Bias and variability—as expressed by (a) average rQ and (b) MAPE—for proposed formula, CAPWAP prediction, modified-Gates formula, modified ENR, Danish formula, PCUBC formula, and Janbu formula.

## 3. THE PILE DRIVING CONTROL SYSTEM (PDCS)

### 3.1 Introduction

Piles are designed to meet the required resistance determined from the structural loads. It is often difficult to predict whether a pile will achieve the required capacity in the field. Overdesign stemming from this uncertainty may lead to projects being uneconomical. Thus, one of the most important goals in the quality assurance (QA) or quality control (QC) of piles is to verify that the capacity of an installed pile matches or slightly exceeds the required value, preferably at the time of installation. In practice, this verification is carried out through static pile load testing, dynamic pile load testing and/or pile driving formulae.

Static pile load testing is the process of measuring the capacity of a pile by loading the pile at a pre-defined loading schedule to an ultimate load. As the loads are measured directly, static pile load tests provide the most reliable measure of pile capacity. However, static pile load testing may be financially unviable for small-scale projects. An indirect estimate of the pile capacity can then be determined through pile driving formulae or dynamic testing (Allen, 2005; Likins, 2015).

Dynamic pile load testing allows the estimation of pile capacity using dynamic measurements of pile acceleration and axial strain at the pile head during pile driving or after pile installation (from dynamic data collected in restrike tests). These tests offer real-time estimation of static pile resistance and are frequently used as a construction monitoring and quality control tool to detect installation problems such as high driving stresses and poor hammer performance. The data acquired during dynamic pile load testing predicts the pile capacity during driving. However, the response of a pile during driving is different from its response under static loading. Thus, the challenge in pile capacity

estimation from dynamic tests is providing an accurate link between the capacity measurements during pile driving and the static resistance (Salgado, 2008). A pile driving control system (PDCS) was developed with the aim of using dynamic measurements to enable engineers to ensure that piling is done economically, without compromising safety. This chapter discusses the instruments generally used in data acquisition and their setup in the field, the procedure adopted for pile capacity estimation, and the operation of the PDCS.

## 3.2 Data Acquisition

In dynamic pile load testing (ASTM D4945-12, 2012), a pair of accelerometers and a pair of strain transducers measure the pile acceleration and axial strain at the pile head, respectively. These are attached to the pile using hardened steel bolts at a distance of at least 1.5 times the pile diameter from the top of the pile to avoid the effects of irregular stress concentrations at the ends of the piles and on diametrically opposite ends of the pile so that the averaged measurements cancel out any effects due to bending. A schematic of the setup for pipe piles and H-piles is shown in Figure 3.1. The specifications of the equipment used is discussed in the subsections ahead. The equipment conforms to the ASTM D4945 (2012) standard.

### *3.2.1 Accelerometers*

The pile driving control unit uses two accelerometers (Figure 3.2a). The accelerometers are mounted using an aluminum block approximately of size 3.5 × 1.5 × 1 in that is bolted on to the pile. The mount serves the purpose of waterproofing the sensor and protecting it from the harsh field conditions.

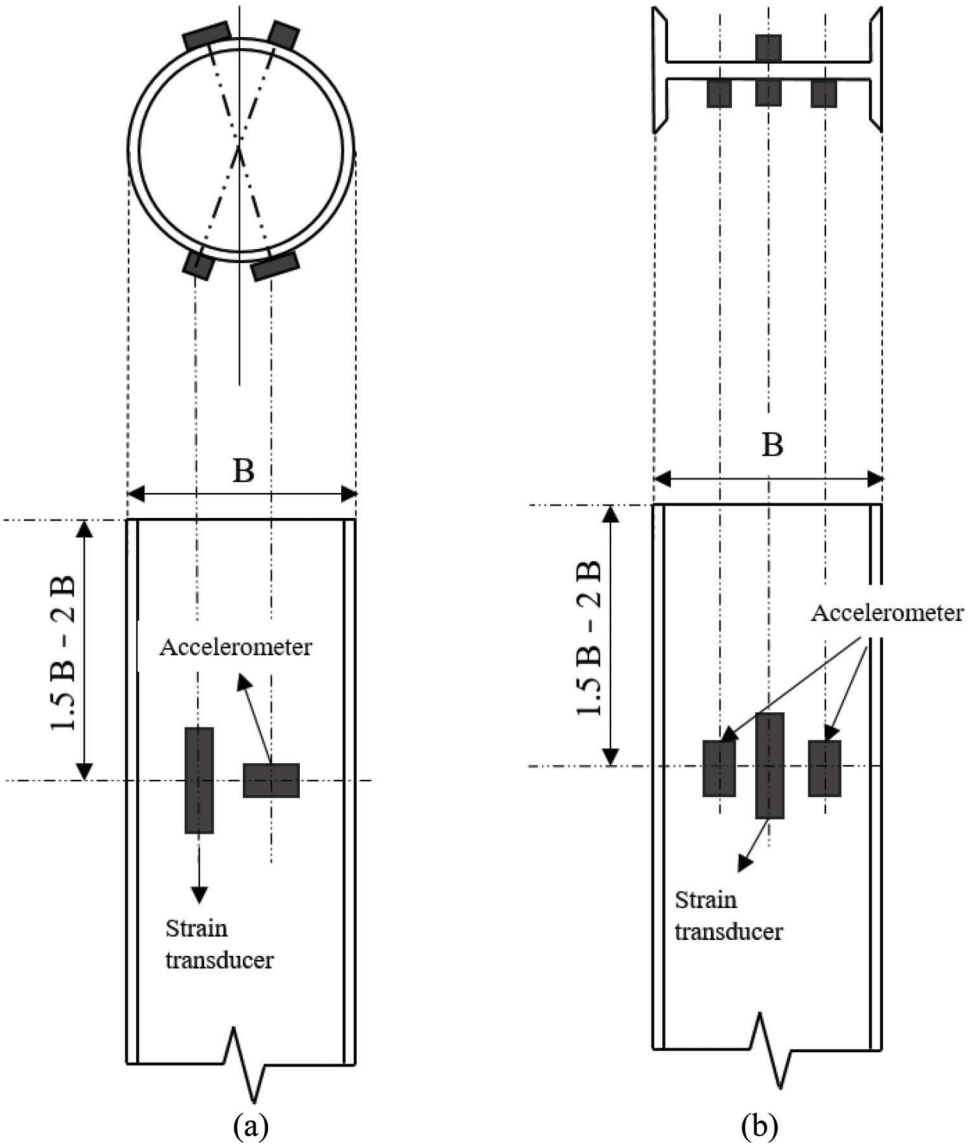


**Figure 3.1** Schematic sketching typical arrangement of strain transducers and accelerometers for dynamic testing in: (a) pipe piles (b) H-piles (after ASTM D4945-12 2012).


**Figure 3.2** Transducers used in the PDCS: (a) accelerometer (b) strain transducer.

*3.2.2 Strain Transducers*

The pile driving control unit uses two strain transducers (Figure 3.2b). These are chosen due to their high sensitivity and ease of installation. The transducers are approximately 4.35 × 1.23 × 0.5 inches in size and are protected by a waterproof aluminum housing. They can be bolted on to the pile using two bolts, each of 3/8″ diameter.

*3.2.3 Data Acquisition System*

The PDCS uses a module for measuring signals from accelerometers and module for measuring signals from strain transducers. Each of these modules contains 4 channels and can collect 50 kS/s/ch at a 24-bit resolution. The high sampling rate and high resolution ensures that a high-quality signal is acquired. Each module is powered from an external chassis that also protects them from the harsh field conditions.

Signals from the sensor, transmitted wirelessly, are collected and processed on a PC placed at a suitable distance from the driving operation. The range of the Wi-Fi signal is dependent on the throughput: the number of samples that can be collected per second from each channel reduces as the distance of the PC from the router increases. For the aforementioned sampling rate, the signals can be collected at distances typical in piling operations.

The power requirements for the devices are met using a combination of batteries and a power bank. The configuration has been chosen to ensure that the PDCS can function continuously for up-to 8 hours in a single charge, and thus function throughout a day's operation in the field. The chassis, modules, and power bank are all enclosed in boxes made from impact-resistant material. The two chassis are enclosed in two boxes each of dimension 11.8″ × 8″ × 4″. The power bank is enclosed in a separate box of dimensions 11.8″ × 5.3″ × 2.8″. The enclosures are padded with foam to dampen the vibrations generated during pile driving.

### 3.3 Data Analysis

In dynamic pile monitoring, the waves recorded from the accelerometer and strain transducers are analyzed to predict the static bearing capacity of the pile. The analysis is typically performed using the Case method (Goble, Likins, & Rausche, 1975), which was developed by making several simplifying assumptions to one-dimensional wave mechanics theory. Although one or more of these assumptions may not be satisfied, correlation studies of the Case method to capacities calculated from static load tests have shown that the Case method is able to roughly approximate the capacity of piles (Rausche, Goble, & Likins, 1985). The advantage offered by the Case method is that of simplicity, allowing capacity predictions to be made in real time on site, thereby serving as an important quality assurance tool. This section provides a brief description of the one-dimensional wave theory and the Case method used for predicting the static pile capacity.

*3.3.1 Wave Mechanics and the Case Method*

A pile can be considered as a slender rod-like linear elastic element with uniform cross-sectional area. The stiffness of the pile is much greater than the stiffness of the surrounding soil. Thus, a wave or pulse generated in the pile from the impact of the hammer primarily travels mostly along the pile. Assuming that the wave is travelling down the pile, the velocity of the particles in a cross section of the pile is given by:

$$v_d(t) = \frac{c}{EA} F(t) = \frac{F(t)}{Z} \tag{3.1}$$

where $v_d(t)$ is the velocity of the particle at time $t$ for a wave travelling down the pile, $E$ is the modulus of elasticity, $A$ is the cross-sectional area, $Z$ is the impedance of the pile defined as the force $F$ experienced by the pile cross section when subjected to a unit velocity $v(t) = 1$ and $c$ is the wave speed, defined by:

$$c = \sqrt{\frac{E}{\rho}} \tag{3.2}$$

where $\rho$ is the mass density of the pile. In contrast, a wave travelling up the pile will have a particle velocity:

$$v_u(t) = -\frac{F(t)}{Z} \tag{3.3}$$

where $v_u(t)$ is the velocity of the particle at time $t$ for a wave travelling up the pile.

A compressive wave travelling down the pile produces a tensile wave of equal magnitude travelling up the pile on reflection from a free end. A free end can thus be considered as a location at which two waves meet: one travelling down the pile and the other travelling up the pile. Using Equations 3.1 and 3.3, the velocity at a free end of a pile can be determined to be twice $v(t)$. The total time taken for a wave to travel down the pile of length $L$ and travel back up again is $2L/c$. Thus, for a finite pile with free ends, the velocity $v$ at the head can be given by:

$$v(t) = \frac{1}{Z}\left(F(t) + 2F\left(t - \frac{2L}{c}\right) + 2F\left(t - \frac{4L}{c}\right) + \cdots\right) \tag{3.4}$$

Resistive forces $R_i(t)$ from the soil acting on the pile at location $z_i$ produce a compressive wave travelling up the pile and a tensile wave travelling down the pile. The particle velocities of each of these waves is given by:

$$v(t) = \frac{R(t)}{2Z}; v(t) = \frac{R(t)}{2Z}(2.20) \tag{3.5}$$

The velocity recorded at the pile head from waves reflected upwards from the soil is simply the sum of velocities from waves reflected upward from locations $i$ along the pile:

$$v(t) = -\frac{1}{Z}\sum_i R_i \times \left(H\left(t - \frac{2z_i}{c}\right) + H\left(t - \frac{2z_i + 2L}{c}\right) + \cdots\right) \tag{3.6}$$

where $H$ is the Heaviside step function defined as:

$$H(t-a) = \begin{pmatrix} 0; t < a \\ 1; t \geq a \end{pmatrix} \tag{3.7}$$

The waves travelling downwards from the soil reactions $R\text{-}_i$ reflect from the pile tip and reach the pile head together with the reflected impact wave. The velocity for these waves is given by:

$$v(t) = -\frac{1}{Z}\sum_i R_i\left(H\left(t - \frac{2L}{c}\right) + H\left(t - \frac{4L}{c}\right) + \cdots\right) \tag{3.8}$$

The net velocity $v(t)$ at the pile head is given by the superposition of velocities defined in Equations 3.4, 3.6, and 3.8. Taking the velocities at time $t = 2L/c$, i.e., on one wave reflection, and subtracting the velocity $v(t)$ from it, we get:

$$v\left(t + \frac{2L}{c}\right) - v(t) = \left[\frac{1}{Z}\left(F\left(t + \frac{2L}{c}\right) + 2F(t) - F(t)\right)\right] + \left[-\frac{1}{Z}\sum_i R_i(H(t))\right] + \left[-\frac{1}{Z}\sum_i R_i(H(t))\right] \tag{3.9}$$

Rearranging the terms in Equation 3.9, we get:

$$R(t) = \frac{1}{2}\left[F(t) + F\left(t + \frac{2L}{c}\right)\right] + \frac{Z}{2}\left[v(t) - v\left(t + \frac{2L}{c}\right)\right] \tag{3.10}$$

The capacity given by Equation 3.10 is the total capacity of the pile during driving. The total capacity can be decomposed as the sum of the static $R_{stat}$ and dynamic capacity $R_{dyn}$:

$$R = R_{dyn} + R_{stat} \tag{3.11}$$

Rausche et al. (1985) assumed that the entire dynamic component of the pile capacity $R_{\mathrm{dyn}}$ was developed at the pile base. This was given as:

$$R_{dyn} = j_c Z v_{toe} \tag{3.12}$$

where $j_c$ is defined as the case damping factor. Thus, for determining the dynamic capacity, the velocity of the toe needs to be calculated. The velocity at the toe is simply the superposition of waves generated at the pile head, Equation 3.4, and the waves generated from the soil resistances, Equation 3.6. This is given as:

$$v\left(t + \frac{L}{c}\right) = v(t) + \frac{1}{Z}[F(t) - R(t)] \tag{3.13}$$

Substituting the velocity calculated using Equation 3.13 to determine the dynamic resistance, Equation 3.12, the static resistance can be determined using Equation 3.11:

$$R_{stat} = \frac{1}{2}\left[(F - Zv)(1 + j_c)\Big|_{t+\frac{2L}{c}} + (F + Zv)(1 - j_c)\Big|_t\right] \tag{3.14}$$

The static resistance obtained from Equation 3.14 is known as the Case resistance.

### 3.4 Using the PDCS

The PDCS has been designed with ease of use as top priority. The PDCS features an intuitive graphic user-interface (GUI) that allows the user collect and analyze data. On starting the PDCS GUI, the main form, as shown in Figure 3.3, will pop up. The operations that can be carried out are listed as tabs on the top left and are highlighted in red. The first tab, 'File,' contains basic operations such as 'Save,' 'Open' and 'Exit'.

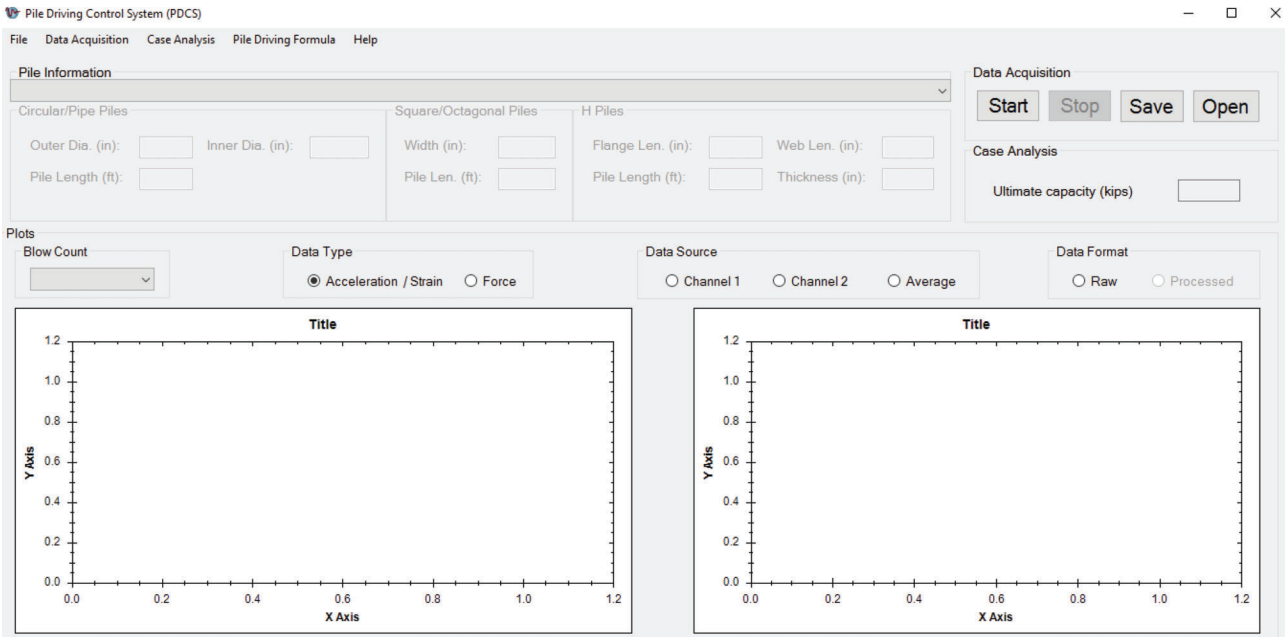


**Figure 3.3** Main form of PDCS.

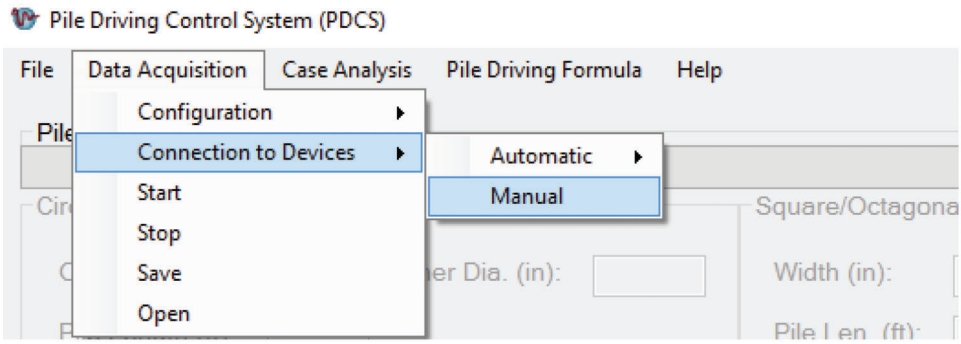


**Figure 3.4** Establishing a wireless connection.

The second tab, 'Data acquisition,' lists all the steps that are related to data acquisition. Acquiring data comprises of four steps:

1. Configuring the devices: this step simply includes entering the calibration factors of the devices.
2. Wirelessly connecting the DAQ: the user can choose to establish a wireless connection between the devices and the computer either automatically or manually (Figure 3.4). The user will be prompted once a successful connection has been able to be established.
3. Acquisition of data: Once a connection has been established, the user should press 'Start' to start acquiring the data. This can be done by clicking 'Start' under the 'Data Acquisition' tab (Figure 3.4) or by clicking the 'Start' button' present on the right side of the main form (Figure 3.3). The system shall now proceed to collect the data. The blow data for each blow during the pile driving process can be seen in two graphs at the bottom of the main form (Figure 3.5). The main form also displays the current blow count on a tab on the left titled 'Blow Count.'
4. Saving the data: Once the data has been acquired, the operator should now press the 'Stop' button present on the right side of the main form or click 'Stop' under the 'Data Acquisition' tab. In the same manner, the operator can save the file for future analysis, if required.

For performing a Case analysis, the operator can go the 'Case Analysis' tab in the main form (Figure 3.6). Performing a Case analysis requires three steps:

1. Input parameters: The parameters required to be input are your blow data and the Case damping factor. For entering the Case damping factor, the GUI will prompt the user for a value in a separate form (Figure 3.7). After entering the value, this form can be closed. For entering the blow data, the user has to select a file that contains stored blow data. This file is generated when the user decides to save the file collected during data acquisition (see step 4 of data acquisition).
2. Starting the Case analysis: Once step 1 is complete, the user can prompt the PDCS to calculate the capacity from the Case method (Equation 3.14) by pressing 'Start' under

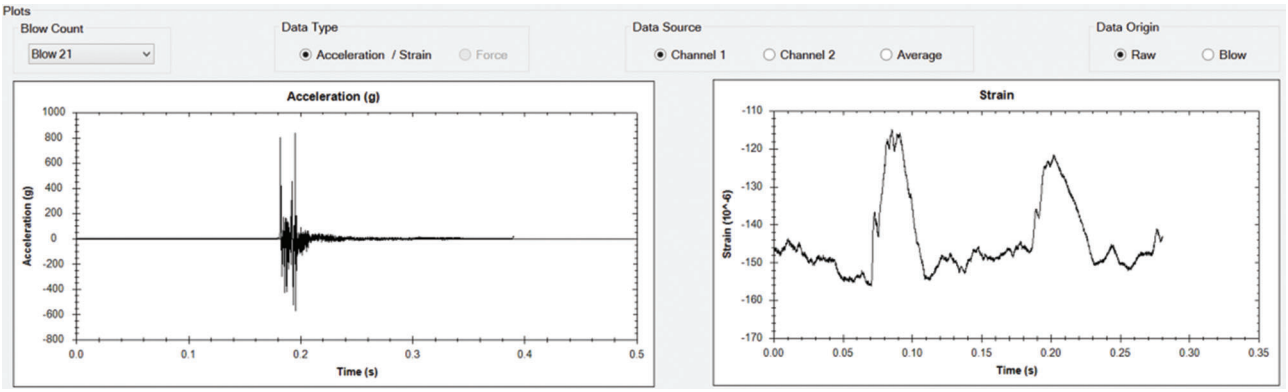


**Figure 3.5** Observation of blows during the pile driving process.

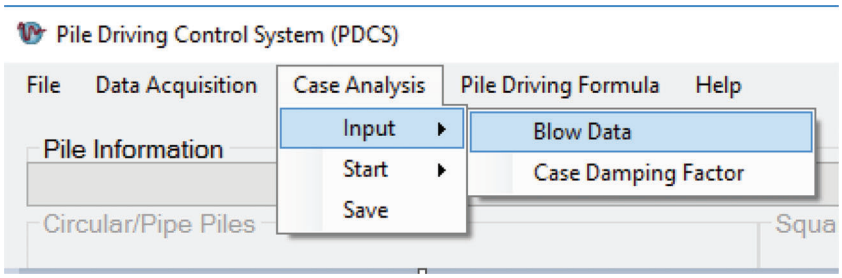


**Figure 3.6** Performing Case analysis in the PDCS.

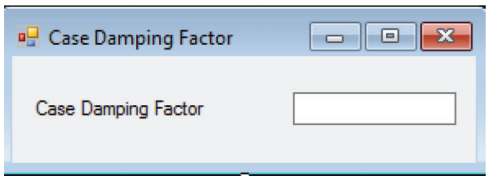


**Figure 3.7** Entering the Case damping factor in the PDCS.

the 'Case Analysis' tab in the main form. The PDCS will then display the capacity to the user.

3. Saving the analysis results: The analysis results can be saved by simply clicking 'Save' under the 'Case Analysis' tab in the main form.

Finally, the operator can choose to predict the capacity using the pile driving formulae developed by Purdue (Equations 2.9 and 2.10). This can be done in three steps:

1. *Opening the 'Pile driving formula' form:* The user should click the 'Pile driving formula' tab in the main form.
2. *Entering required values:* In the 'Pile driving formula' form, the operator should select and enter the parameter values (Figure 3.8).
3. *Starting the analysis:* The user should press the 'Start' button in the 'Pile driving formula' form and the analysis results will be displayed at the white text space at the bottom of the form.

Once all operations required have been performed, the operator can exit the system by selecting 'File' and then clicking on 'Exit' in the main form, or by simply pressing the 'X' button on the top right of the screen.

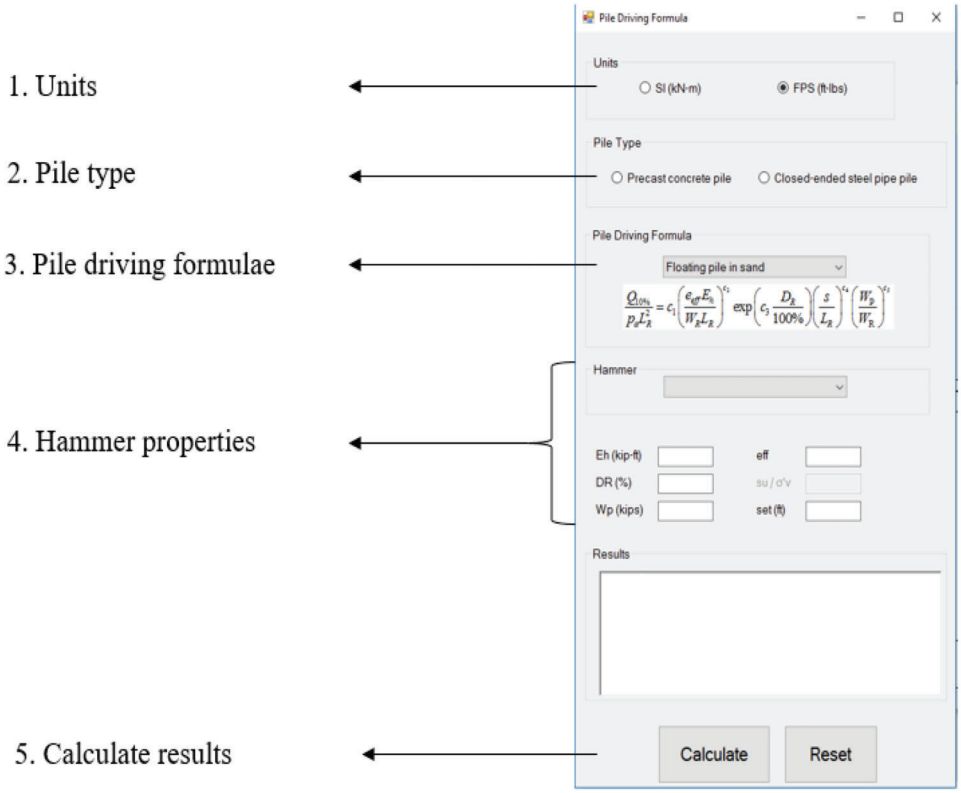


**Figure 3.8** Parameters in the pile driving formula form.

## 4. SUMMARY AND CONCLUSIONS

The present study details the configuration and operation of the pile driving control system (PDCS), an integrated system designed to collect data and to estimate pile capacities. Pile capacities can be predicted either using existing methods such as the Case method or through pile driving formulae. These formulae are developed for two pile types and five soil profiles, and have been shown to outperform existing formulae based on several well-documented case studies containing full-scale instrumented pile load tests. The PDCS is a prototype system that works only in a fully integrated manner. Additional testing of the prototype system for a variety of hammers, pile types and soil profiles should be done to assess the performance and to increase the efficacy and robustness of the system.

## REFERENCES


Allen, T. (2005). *Development of the WSDOT pile-driving formula and its calibration for load and resistance factor design (LRFD)*. Olympia, WA: Washington State Department of Transportation.

Altaee, A., Fellenius, B. H., & Evgin, E. (1992). Axial load transfer for piles in sand. I. Tests on an instrumented precast pile. *Canadian Geotechnical Journal*, *29*(1), 11–20. https://doi.org/10.1139/t92-002

ASTM D4945-12. (2012). *Standard test method for high-strain dynamic testing of deep foundations*. West Conshohocken, PA: ASTM International. https://doi.org/10.1520/D4945-12

Basu, P., Prezzi, M., Salgado, R., & Chakraborty, T. (2014). Shaft resistance and setup factors for piles jacked in clay. *Journal of Geotechnical and Geoenvironmental Engineering*, *140*(3), 4013026-1–004013026-16. https://doi.org/10.1061/(ASCE)GT.1943-5606.0001018

Bowles, E. J. (1996). *Foundation analysis and design*. New York, NY: McGraw-Hill.

ENR. (1965). Michigan pile test program test results are released. *Engineering News-Record, May 20*, 26–28, 33–34.

Fellenius, B. H., & Samson, L. (1976). Testing of drivability of concrete piles and disturbance to sensitive clay. *Canadian Geotechnical Journal*, *13*(2), 139–160. https://doi.org/10.1139/t76-015

Fellenius, B. H., Harris, D. E., & Anderson, D. G. (2004). Static loading test on a 45 m long pipe pile in Sandpoint, Idaho. *Canadian Geotechnical Journal*, *41*(4), 613–628. https://doi.org/10.1139/t04-012

Goble, G. G., Likins, G. E., & Rausche, F. (1975). *Bearing capacity of piles from dynamic measurements*. Cleveland, OH: Ohio Department of Transportation.

GRL Engineers, Inc. (1997). Case Pile Wave Analysis Program (CAPWAP) [Software]. Cleveland, OH: GRL Engineers, Inc.

Han, F., Prezzi, M., Salgado, R., & Zaheer, M. (2016). Assessment of the axial resistance of closed-ended steel pipe piles driven in multilayered soil. *Journal of Geotechnical and Geoenvironmental Engineering*, *143*(3), 04016102-1–04016102-16.

Holeyman, A. E. (1985).Dynamic non-linear skin friction of piles. In *Proceedings of the International Symposium on Penetrability and Drivability of Piles, San Francisco, 10 August, 1985* (Vol. 1, pp. 173–176). http://www.vulcanhammer.info/drivability/Holeyman_1985_Dynamic_non-linear_skin_friction_of_piles.pdf

INDOT. (2016). *2016 standard specifications*. Indianapolis, IN: Indiana Department of Transportation. Retrieved from http://www.in.gov/dot/div/contracts/standards/book/sep15/sep.htm

Ismael, N. F. (1999). Analysis of load tests on piles driven through calcareous desert sands. *Journal of Geotechnical and Geoenvironmental Engineering*, *125*(10), 905–908. https://doi.org/10.1061/(ASCE)1090-0241(1999)125:10(905)

Kim, D., Bica, A. V., Salgado, R., Prezzi, M., & Lee, W. (2009). Load testing of a closed-ended pipe pile driven in multilayered soil. *Journal of Geotechnical and Geoenvironmental Engineering*, *134*(4), 463–473. https://doi.org/10.1061/(ASCE)1090-0241(2009)135:4(463)

Kulesza, R. L., & Fellenius, B. H. (2012). Design and testing of piles on a telecommunications project in Morocco. In M. H. Hussein, K. R. Massarsch, G. E. Likins, & R. D. Holtz (Eds.), *Full-scale testing and foundation design* (GeoCongress 2012, pp. 452–470). Reston, VA: American Society of Civil Engineers. https://doi.org/10.1061/9780784412084.0033

Lam, J. (2007). *Termination criteria for high-capacity jacked and driven steel H-piles in Hong Kong* (Doctoral dissertation). Hong Kong, China: University of Hong Kong.

Likins, G. (2015). *Pile testing—State-of-the-art*. Paper presented at the 8th Seminar on Special Foundations Engineering and Geotechnics, São Paulo, Brazil, June.

Likins, G. E., Fellenius, B. H., & Holtz, R. D. (2012). Pile driving formulas: Past and present. In M. H. Hussein, K. R. Massarsch, G. E. Likins, & R. D. Holtz (Eds.), *Full-scale testing and foundation design: Honoring Bengt H. Fellenius* (GeoCongress 2012, pp. 737–753). Reston, VA: American Society of Civil Engineers. https://doi.org/10.1061/9780784412084.0051

Lim, P. C., & Broms, B. B. (1990). Influence of pile driving hammer performance on driving criteria. *Geotechnical Engineering*, *21*(1), 63–69.

Martin, R. E., Seli, J. J., Powell, G. W., & Bertoulin, M. (1987). Concrete pile design in Tidewater Virginia. *Journal of Geotechnical Engineering*, *113*(6), 568–585. https://doi.org/10.1061/(ASCE)0733-9410(1987)113:6(568)

McVay, M. C., Birgisson, B., Zhang, L., Perez, A., & Putcha, S. (2000). Load and resistance factor design (LRFD) for driven piles using dynamic methods—a Florida perspective. *Geotechnical Testing Journal*, *23*(1), 55–66. https://doi.org/10.1520/GTJ11123J

Meyerhof, G. G., & Murdock, L. J. (1953). An investigation of the bearing capacity of some bored and driven piles in London clay. *Géotechnique*, *3*(7), 267–282. https://doi.org/10.1680/geot.1953.3.7.267

Mostafa, Y. E. (2011). Onshore and offshore pile installation in dense soils. *Journal of American Science*, *7*(7) 549–563. https://doi.org/10.7537/marsjas070711.80

Olson, R. E., & Flaate, K. S. (1967). Pile-driving formulas for friction piles in sand. *Journal of the Soil Mechanics and Foundations Division, 93*(SM6), 279–296.

Paik, K., Salgado, R., Lee, J., & Kim, B. (2003). Behavior of open- and closed-ended piles driven into sands. *Journal of Geotechnical and Geoenvironmental Engineering*, *129*(4), 296–306. https://doi.org/10.1061/(ASCE)1090-0241(2003)129:4(296)

Randolph, M. F., & Simons, H. A. (1986). An improved soil model for one-dimensional pile driving analysis. In *Proceedings of the Third International Conference on Numerical Methods in Offshore Piling* (pp. 3–17). Nantes, France: Editions Technip.

Rausche, F. (2000). Pile driving equipment: Capabilities and properties. In S. Niyama & J. Beim (Eds.), *Proceedings of the 6th International Conference on the Application of Stress-Wave Theory to Piles; Quality Assurance on Land and Offshore Piling* (pp. 75–90). Rotterdam, Netherlands: A. A. Balkema.

Rausche, F., Goble, G. G., & Likins, G. E. (1985). Dynamic determination of pile capacity. *Journal of Geotechnical Engineering*, *111*(3), 367–383. https://doi.org/10.1061/(ASCE)0733-9410(1985)111:3(367)

Salgado, R. (2008). *The engineering of foundations*. New York, NY: McGraw-Hill.

Salgado, R., & Prezzi M. (2007). Computation of cavity expansion pressure and penetration resistance in sands. *International Journal of Geomechanics*, *7*(4), 251–265. https://doi.org/10.1061/(ASCE)1532-3641(2007)7:4(251)

Salgado, R., & Zhang, Y. (2012). *Use of pile driving analysis for assessment of axial load capacity of piles* (Joint Transportation Research Program Publication No. FHWA/IN/JTRP-2012/11). West Lafayette, IN: Purdue University. https://doi.org/10.5703/1288284314671

Salgado, R., Loukidis, D., Abou-Jaoude, G., & Zhang, Y. (2015). The role of soil stiffness non-linearity in 1D pile driving simulations. *Géotechnique*, *65*(3), 169–187. https://doi.org/10.1680/geot.13.P.124

Salgado, R., Woo, S. I., & Kim, D. (2011). *Development of load and resistance factor design for ultimate and serviceability limit states of transportation structure foundations* (Joint Transportation Research Program Publication No. FHWA/IN/JTRP-2011/03). West Lafayette, IN: Purdue University. https://doi.org/10.5703/1288284314618

Salgado, R., Zhang, Y., Abou-Jaoude, G., Loukidis, D., & Bisht, V. (2017). Pile driving formulas based on pile wave equation analyses. *Computers and Geotechnics*, *81*, 307–321. https://doi.org/10.1016/j.compgeo.2016.09.004

Skempton, A. W. (1986). Standard penetration test procedures and the effects in sands of overburden pressure, relative density, particle size, ageing and overconsolidation. *Géotechnique*, *36*(3), 425–447. https://doi.org/10.1680/geot.1986.36.3.425

Terzaghi, K. (1942). Discussions on the progress report of the committee on the bearing value of pile foundations. *Proceedings of the American Society of Civil Engineers*, *68*(2), 311–323.

Yen, T.-L., Lin, H., Chin, C.-T., & Wang, R. F. (1989). Interpretation of instrumented driven steel pipe piles. In F. H. Kulhawy (Ed.), *Foundation engineering: Current principles and practices—Volume 2* (Geotechnical Special Publication No. 22, pp. 25–29). Reston, VA: American Society of Civil Engineers.

## About the Joint Transportation Research Program (JTRP)

On March 11, 1937, the Indiana Legislature passed an act which authorized the Indiana State Highway Commission to cooperate with and assist Purdue University in developing the best methods of improving and maintaining the highways of the state and the respective counties thereof. That collaborative effort was called the Joint Highway Research Project (JHRP). In 1997 the collaborative venture was renamed as the Joint Transportation Research Program (JTRP) to reflect the state and national efforts to integrate the management and operation of various transportation modes.

The first studies of JHRP were concerned with Test Road No. 1—evaluation of the weathering characteristics of stabilized materials. After World War II, the JHRP program grew substantially and was regularly producing technical reports. Over 1,600 technical reports are now available, published as part of the JHRP and subsequently JTRP collaborative venture between Purdue University and what is now the Indiana Department of Transportation.

Free online access to all reports is provided through a unique collaboration between JTRP and Purdue Libraries. These are available at: http://docs.lib.purdue.edu/jtrp

Further information about JTRP and its current research program is available at: http://www.purdue.edu/jtrp

## About This Report

An open access version of this publication is available online. This can be most easily located using the Digital Object Identifier (doi) listed below. Pre-2011 publications that include color illustrations are available online in color but are printed only in grayscale.

The recommended citation for this publication is:

Salgado, R., Bisht, V., & Prezzi, M. (2017). *Pile driving analysis for pile design and quality assurance* (Joint Transportation Research Program Publication No. FHWA/IN/JTRP-2017/15). West Lafayette, IN: Purdue University. https://doi.org/10.5703/1288284316514